Oz, M. C., Hicklin, D. J., Witte, L., Moore, M. A., and Rafii, S. (2000) *Blood* **95,** 952–958
9. Rehman, J., Li, J., Orschell, C. M., and March, K. L. (2003) *Circulation* **107,** 1164–1169
10. Kocher, A. A., Schuster, M. D., Szabolcs, M. J., Takuma, S., Burkhoff, D., Wang, J., Homma, S., Edwards, N. M., and Itescu, S. (2001) *Nat. Med.* **7,** 430–436
11. Bahlmann, F. H., De Groot, K., Spandau, J. M., Landry, A. L., Hertel, B., Duckert, T., Boehm, S. M., Menne, J., Haller, H., and Fliser, D. (2004) *Blood* **103,** 921–926
12. Bahlmann, F. H., DeGroot, K., Duckert, T., Niemczyk, E., Bahlmann, E., Boehm, S. M., Haller, H., and Fliser, D. (2003) *Kidney Int.* **64,** 1648–1652
13. Heeschen, C., Aicher, A., Lehmann, R., Fichtlscherer, S., Vasa, M., Urbich, C., Mildner-Rihm, C., Martin, H., Zeiher, A. M., and Dimmeler, S. (2003) *Blood* **102,** 1340–1346
14. Dimmeler, S., Aicher, A., Vasa, M., Mildner-Rihm, C., Adler, K., Tiemann, M., Rutten, H., Fichtlscherer, S., Martin, H., and Zeiher, A. M. (2001) *J. Clin. Investig.* **108,** 391–397
15. Llevadot, J., Murasawa, S., Kureishi, Y., Uchida, S., Masuda, H., Kawamoto, A., Walsh, K., Isner, J. M., and Asahara, T. (2001) *J. Clin. Investig.* **108,** 399–405
16. Kaushansky, K., Lok, S., Holly, R. D., Broudy, V. C., Lin, N., Bailey, M. C., Forstrom, J. W., Buddle, M. M., Oort, P. J., Hagen, F. S., Roth, G. J., Papayannopoulou, T., and Foster, D. C. (1994) *Nature* **369,** 568–571
17. Fox, N., Priestley, G., Papayannopoulou, T., and Kaushansky, K. (2002) *J. Clin. Investig.* **110,** 389–394
18. Kimura, S., Roberts, A. W., Metcalf, D., and Alexander, W. S. (1998) *Proc. Natl. Acad. Sci. U. S. A.* **95,** 1195–1200
19. Sitnicka, E., Lin, N., Priestley, G. V., Fox, N., Broudy, V. C., Wolf, N. S., and Kaushansky, K. (1996) *Blood* **87,** 4998–5005
20. Brizzi, M. F., Battaglia, E., Montrucchio, G., Dentelli, P., Del Sorbo, L., Garbarino, G., Pegoraro, L., and Camussi, G. (1999) *Circ. Res.* **84,** 785–796
21. Kaushansky, K., Lin, N., Grossmann, A., Humes, J., Sprugel, K. H., and Broudy, V. C. (1996) *Exp. Hematol.* **24,** 265–269
22. Broudy, V. C., Lin, N. L., and Kaushansky, K. (1995) *Blood* **85,** 1719–1726
23. Kaushansky, K., Broudy, V. C., Grossmann, A., Humes, J., Lin, N., Ren, H. P., Bailey, M. C., Papayannopoulou, T., Forstrom, J. W., and Sprugel, K. H. (1995) *J. Clin. Investig.* **96,** 1683–1687
24. Kobayashi, M., Laver, J. H., Kato, T., Miyazaki, H., and Ogawa, M. (1995) *Blood* **86,** 2494–2499
25. Kanayasu-Toyoda, T., Yamaguchi, T., Oshizawa, T., and Hayakawa, T. (2003) *J. Cell. Physiol.* **195,** 119–129
26. Hur, J., Yoon, C. H., Kim, H. S., Choi, J. H., Kang, H. J., Hwang, K. K., Oh, B. H., Lee, M. M., and Park, Y. B. (2004) *Arterioscler. Thromb. Vasc. Biol.* **24,** 288–293
27. Yoon, C. H., Hur, J., Park, K. W., Kim, J. H., Lee, C. S., Oh, I. Y., Kim, T. Y., Cho, H. J., Kang, H. J., Chae, I. H., Yang, H. K., Oh, B. H., Park, Y. B., and Kim, H. S. (2005) *Circulation* **112,** 1618–1627
28. Miyakawa, Y., Rojnuckarin, P., Habib, T., and Kaushansky, K. (2001) *J. Biol. Chem.* **276,** 2494–2502
29. Drachman, J. G., Sabath, D. F., Fox, N. E., and Kaushansky, K. (1997) *Blood* **89,** 483–492
30. Kirito, K., Watanabe, T., Sawada, K., Endo, H., Ozawa, K., and Komatsu, N. (2002) *J. Biol. Chem.* **277,** 8329–8337
31. Li, A., Dubey, S., Varney, M. L., Dave, B. J., and Singh, R. K. (2003) *J. Immunol.* **170,** 3369–3376
32. Mizukami, Y., Jo, W. S., Duerr, E. M., Gala, M., Li, J., Zhang, X., Zimmer, M. A., Iliopoulos, O., Zukerberg, L. R., Kohgo, Y., Lynch, M. P., Rueda, B. R., and Chung, D. C. (2005) *Nat. Med.* **11,** 992–997
33. Salcedo, R., Ponce, M. L., Young, H. A., Wasserman, K., Ward, J. M., Kleinman, H. K., Oppenheim, J. J., and Murphy, W. J. (2000) *Blood* **96,** 34–40
34. Lin, Y., Weisdorf, D. J., Solovey, A., and Hebbel, R. P. (2000) *J. Clin. Investig.* **105,** 71–77
35. Assmus, B., Schachinger, V., Teupe, C., Britten, M., Lehmann, R., Dobert, N., Grunwald, F., Aicher, A., Urbich, C., Martin, H., Hoelzer, D., Dimmeler, S., and Zeiher, A. M. (2002) *Circulation* **106,** 3009–3017
36. Kalka, C., Masuda, H., Takahashi, T., Kalka-Moll, W. M., Silver, M., Kearney, M., Li, T., Isner, J. M., and Asahara, T. (2000) *Proc. Natl. Acad. Sci. U. S. A.* **97,** 3422–3427
37. Kawamoto, A., Gwon, H. C., Iwaguro, H., Yamaguchi, J. I., Uchida, S., Masuda, H., Silver, M., Ma, H., Kearney, M., Isner, J. M., and Asahara, T. (2001) *Circulation* **103,** 634–637
38. Kirito, K., Fox, N., Komatsu, N., and Kaushansky, K. (2005) *Blood* **105,** 4258–4263
39. Kelemen, E., Cserhati, I., and Tanos, B. (1958) *Acta Haematol. (Basel)* **20,** 350–355
40. Yamamoto, S. (1957) *Acta Haematol. Jpn.* **20,** 163
41. Kanayasu-Toyoda, T., Yamaguchi, T., Uchida, E., and Hayakawa, T. (1999) *J. Biol. Chem.* **274,** 25471–25480
42. Yamaguchi, T., Mukasa, T., Uchida, E., Kanayasu-Toyoda, T., and Hayakawa, T. (1999) *J. Biol. Chem.* **274,** 15575–15581
43. Miyamoto, K., Nishigami, K., Nagaya, N., Akutsu, K., Chiku, M., Kamei, M., Soma, T., Miyata, S., Higashi, M., Tanaka, R., Nakatani, T., Nonogi, H., and Takeshita, S. (2006) *Circulation* **114,** 2679–2684
44. George, J., Afek, A., Abashidze, A., Shmilovich, H., Deutsch, V., Kopolovich, J., Miller, H., and Keren, G. (2005) *Arterioscler. Thromb. Vasc. Biol.* **25,** 2636–2641

Leukemia (2007), 1–10

www.nature.com/leu

ORIGINAL ARTICLE

Proteome analyses of the growth inhibitory effects of NCH-51, a novel histone deacetylase inhibitor, on lymphoid malignant cells

T Sanda[1,2], T Okamoto[1], Y Uchida[1], H Nakagawa[3], S Iida[2], S Kayukawa[2], T Suzuki[3], T Oshizawa[4], T Suzuki[4], N Miyata[3] and R Ueda[2]

[1]Department of Molecular and Cellular Biology, Nagoya City University Graduate School of Medical Sciences, Nagoya, Japan; [2]Department of Internal Medicine and Molecular Science, Nagoya City University Graduate School of Medical Sciences, Nagoya, Japan; [3]Department of Organic and Medicinal Chemistry, Nagoya City University Graduate School of Pharmaceutical Sciences, Nagoya, Japan and [4]Department of Cellular and Gene Therapy Products, National Institute of Health Sciences, Tokyo, Japan

Recent reports showing successful inhibition of cancer and leukemia cell growth using histone deacetylase inhibitor (HDACi) compounds have highlighted the potential use of HDACi as anti-cancer agents. However, high incidence of toxicity and low stability *in vivo* were observed with hydroxamic acid-based HDACi such as suberoylanilide hydroxamic acid (SAHA), thus limiting its clinical applicability. In this study, we found that a novel non-hydroxamate HDACi NCH-51 could inhibit the cell growth of a variety of lymphoid malignant cells through apoptosis induction, more effectively than SAHA. Activation of caspase-3, -8 and -9, but not -7 was detected after the treatment with NCH-51. Gene expression profiles showed that NCH-51 and SAHA similarly upregulated *p21* and downregulated anti-apoptotic molecules including *survivin*, *bcl-w* and *c-FLIP*. Proteome analysis using two-dimensional electrophoresis revealed that NCH-51 upregulated anti-oxidant molecules including peroxiredoxin 1 and 2 and glutathione *S*-transferase at the protein level. Interestingly, NCH-51 induced reactive oxygen species (ROS) after 8 h whereas SAHA continuously declined ROS. Pretreatment with an antioxidant, *N*-acetyl-L-cysteine, abolished the cytotoxicity of NCH-51. These findings suggest that NCH-51 exhibits cytotoxicity by sustaining ROS at the higher level greater than SAHA. This study indicates the therapeutic efficacy of NCH-51 and novel insights for anti-HDAC therapy.
Leukemia advance online publication, 9 August 2007; doi:10.1038/sj.leu.2404902
Keywords: histone deacetylase; apoptosis; reactive oxygen species; peroxiredoxin

Introduction

Histone deacetylase (HDAC) is responsible for deacetylation of histone or non-histone substrates.[1–3] Deacetylation of histone converts local chromatin into repressive configuration, resulting in the transcriptional repression.[2,3] The aberrant recruitment of HDAC is closely associated with leukemogenesis through silencing of expression of the genes involved in hematopoietic cell differentiation.[4] In addition, subsequent studies demonstrated that the malignant phenotypes of solid tumors could be ascribed to the aberrant activation of HDAC and deacetylation of the histone proteins adjacent to tumor suppressor genes.[5,6] Thus, a number of small-molecule HDAC inhibitors (HDACi) have been developed as anti-cancer agents.[1,7] In fact, HDACi compounds were shown to induce cell cycle arrest, differentiation and apoptosis in a variety of malignant cells.[1,7]

Suberoylanilide hydroxamic acid (SAHA) (also known as vorinostat) belongs to a hydroxamic acid-based hybrid polar compound and is a prototypic compound of HDACi.[7] Phase I clinical trials with refractory solid tumors and hematological malignancies by SAHA revealed frequent toxicities including dehydration, fatigue, diarrhea, anorexia and cytopenia, in spite of significant clinical benefits.[8] In addition, a poor pharmacokinetics of SAHA was noted.[8] Other hydroxamic acid-based derivatives showed similar therapeutic profiles.[9,10] Thus, we have attempted to develop a non-hydroxamate HDACi to overcome these problems. A novel HDACi NCH-51 was designed based on SAHA by replacement of the hydroxamic acid by acylated thiol group. NCH-51 could inhibit HDACs as strongly as SAHA and inhibited the cell growth of various solid tumor cell lines *in vitro* (mean IC_{50} values of NCH-51 and SAHA are 3.8 and 3.7 μM, respectively).[11] Unlike SAHA, NCH-51 is stable in human plasma at the remaining rate of approximately 51% after 24 h of administration (unpublished data).

Recent findings suggest that HDACi may have additional effects other than transcriptional interference. Although it is well established that HDACi upregulates gene expression of tumor suppressors such as *p21* through histone hyperacetylation,[12–14] HDACi does not always upregulate gene expression but induces malignant cell death by downregulating gene expression such as anti-apoptotic genes. In addition, some HDACi compounds exhibited anti-cancer effects through acetylation of non-histone substrates such as heat-shock protein 90 (HSP90),[15] α-tubulin,[16] p53[17] and nuclear factor-κB.[18] For example, Bali *et al.*[15] reported that HDACi caused leukemia cell death by hyperacetylation of HSP90. Hideshima *et al.*[19] demonstrated that tubacin, a specific HDAC6 inhibitor, was effective in augmenting cell death mediated by bortezomib, a proteasome inhibitor, by inhibiting the protein degradation through blocking aggresome activity. Thus, the cell growth inhibitory action of HDACi could be exhibited at the protein expression level.

Here we demonstrate the therapeutic efficacy of NCH-51 on lymphoid malignant cells. NCH-51 induced cell death, more strongly than SAHA. We analyzed the protein expression profiles and found that NCH-51 modulated the expression of antioxidant molecules at the protein level. NCH-51 sustained the intracellular reactive oxygen species (ROS) greater than SAHA.

Correspondence: Professor T Okamoto, Department of Molecular and Cellular Biology, Nagoya City University Graduate School of Medical Sciences, 1 Kawasumi, Mizuho-cho, Mizuho-ku, Nagoya, Aichi 467-8601, Japan.
E-mail: tokamoto@med.nagoya-cu.ac.jp
Received 22 March 2007; revised 6 June 2007; accepted 11 July 2007

a

Cell type		Cell line name	24h		72h	
			SAHA	NCH-51	SAHA	NCH-51
T-cell	T-ALL	Jurkat	[illegible]	0.72	0.63	0.75
	ATL	MT-2	>30.00	[illegible]	0.54	2.08
		ATL-102	>30.00	[illegible]	3.70	2.25
		ED-40515 (-)	[illegible]	0.94	0.90	0.76
	CLL	MEC2	>30.00	0.71	0.79	0.87
		MO1043	>30.00	[illegible]	0.76	0.79
B-cell	BL	Raji	>30.00	1.65	0.84	0.71
		Daudi	>30.00	>30.00	[illegible]	[illegible]
	MM	U266	[illegible]	1.36	0.53	0.66
		XG7	>30.00	[illegible]	0.73	1.11
		KMS	>30.00	>30.00	1.35	3.49
		ILKM-2	1.41	1.11	0.61	0.66
		RPMI8226	3.72	2.92	2.92	2.72

Growth inhibition (%)
80-100
60-80
40-60
20-40
0-20
Each Value means IC_{50}

b

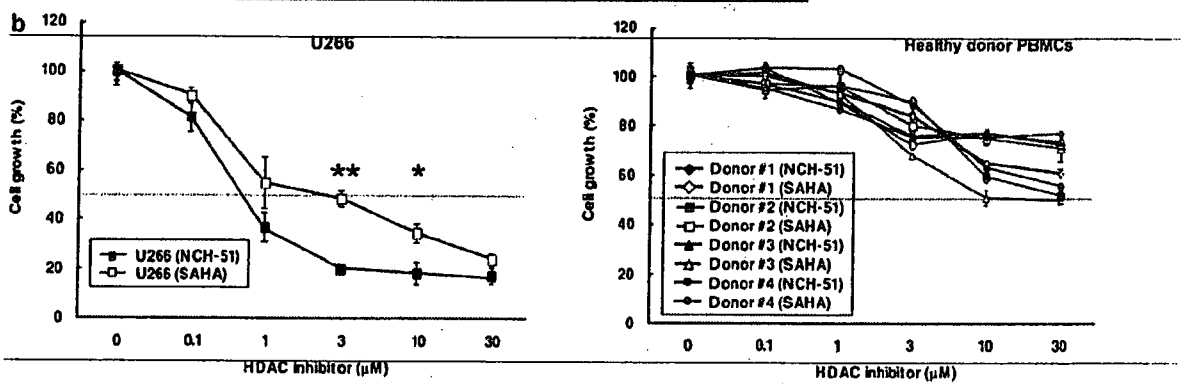

c

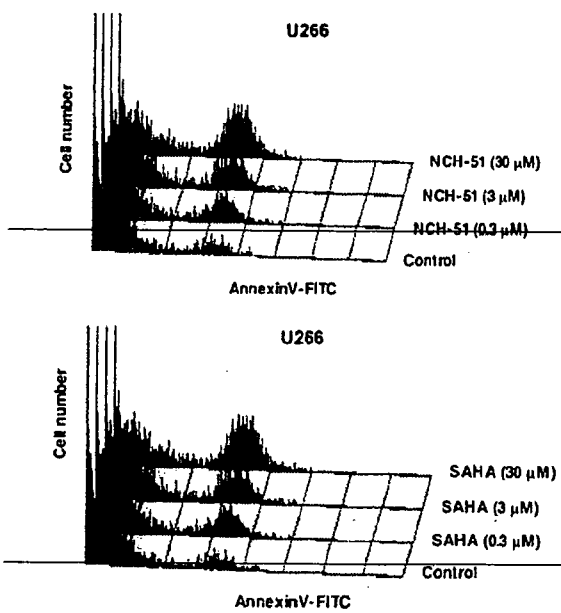

d

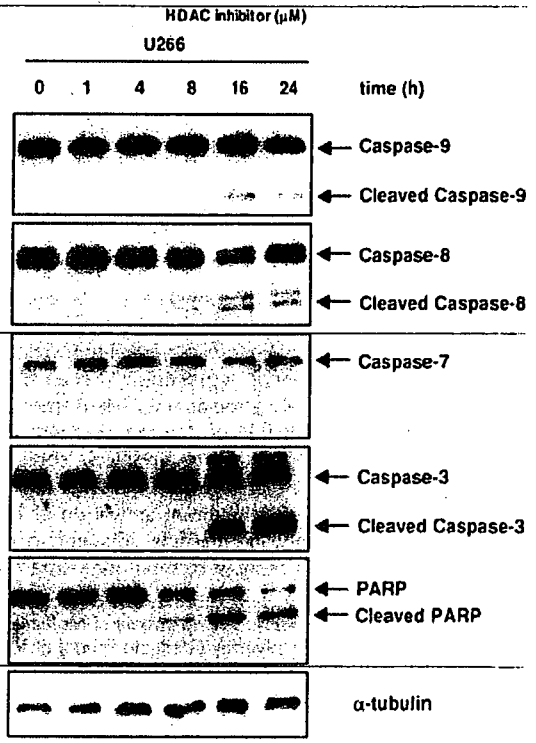

Materials and methods

Cell lines and reagents

A human acute T-cell leukemia cell line, Jurkat, ATL cell lines, MT-2, ATL-102 and ED-40515(−), chronic lymphocytic leukemia cell lines, MEC2 and MO1043, Burkitt's lymphoma cell lines, Raji and Daudi and multiple myeloma cell lines, U266, XG7, KM5, ILKM-2 and RPMI-8226 were used in this study as described previously.[20–24] For normal controls, peripheral blood mononuclear cells (PBMCs) were obtained from four independent healthy donors upon informed consent after the approval of Institutional Ethical Committee. All cells were cultured in RPMI-1640 medium, supplemented with 10% fetal bovine serum at 37°C in a 5% CO_2 incubator. NCH-51, a novel non-hydroxamate HDACi, and SAHA, a conventional hydroxamate HDACi, were synthesized by us as described previously.[11] NCH-51 and SAHA were dissolved in dimethyl sulfoxide at 50 mM and stored at −20°C. An antioxidant compound *N*-acetyl-L-cysteine (NAC) was purchased from Sigma (St Louis, MS, USA).

Growth inhibition assay

Growth inhibitory effect of HDACi was determined using 3-(4,5-dimethylthiazol-2-yl)-2,5-diphenyltetrazolium bromide assay (Sigma) as described previously.[25] Briefly, approximately $1–10 \times 10^4$ cells per 100 μl were cultured in 96-well plate in triplicates at 37°C. Optical densities (OD) at 570 and 630 nm were measured with a multiplate reader. Cell growth (%) was calculated as follows: (OD_{630}–OD_{570} of the samples/OD_{630}–OD_{570} of the control) × 100.

Apoptosis and cell cycle analysis

Apoptosis and cell cycle analyses were performed as described previously.[20] For apoptosis analysis, the cells were treated with or without HDACi for 18 h, and incubated with fluorescein isothiocyanate (FITC)-conjugated annexin V (MBL, Nagoya, Japan). The cell numbers of annexin V-positive cells were analyzed by flowcytometry (FACScan, BD Bioscience, San Jose, CA, USA) and CellQuest analysis program (BD Bioscience). For cell cycle analysis, the cells were incubated with or without HDACi for 24 h, washed with cold phosphate-buffered saline (PBS), and fixed with 70% ethanol. After incubation with RNase A (Qiagen, Alameda, CA, USA), the cell pellets were resuspended in PBS containing propidium iodide (Sigma). DNA content of each cell preparation was analyzed by flowcytometry.

Protein extraction for proteome analysis

Proteome analysis was performed according to Seike *et al*.[26] U266 cells were incubated with or without 3 μM NCH-51 for 18 h. The cell pellets were washed with cold PBS and then treated with 10%trichloroacetic acid for 30 min on ice. After washing with PBS, the pellets were collected and resuspended in lysis buffer (30 mM Tris–HCl (pH, 8.5), 7 M urea, 2 M thiourea, 3% 3-((3-chlamidopropyl) dimethylammonio)-1-propanesulfonic acid and 1% Triton X-100). Samples were then subjected to a Dounce homogenizer for 30 strokes and sonicated for 5 min in a sonicator (UCW-201, Cosmobio Co. Ltd., Tokyo, Japan). After incubation for 30 min, the samples were centrifuged at 10 000 × *g* for 30 min followed by ultracentrifugation at 100 000 × *g* for 1 h, and the supernatants were collected. Protein concentration was determined by 2D-Quant kit (GE Healthcare Bio-Sciences Corp., Piscataway, NJ, USA). Fifty micrograms of each protein extract, adjusted to pH 8.5, were labeled with 200 pmol of minimal dye CyDye (GE Healthcare Bio-Sciences Corp.). NCH-51-treated samples and untreated control proteins were labeled with Cy3 and Cy5, respectively. Internal control, consisting of half part of each paired sample was labeled with Cy2. Labeling reaction was stopped with the addition of 0.2 mM L-lysine (Sigma) for 10 min on ice. Each labeled sample was mixed into one tube and then incubated with an equal amount of lysis buffer for 10 min on ice. The final volume was adjusted to 450 μl with DeStreak Rehydration Solution and 0.5% IPG buffer (GE Healthcare Bio-Sciences Corp.).

Two-dimensional (2D) electrophoresis and image analysis

An immobilized pH gradient gel Immobiline DryStrip (GE Healthcare Bio-Sciences Corp.), with non-linear pH values (3–10), was rehydrated with the labeled protein samples at 20°C for 12 h. Isoelectric focusing was performed using IPGphor (GE Healthcare Bio-Sciences Corp.) at 20°C for total 65 000 khT. Immobiline DryStrips were then equilibrated for 15 min in the buffer (6 M urea, 1.5 M Tris–HCl (pH 8.8), 30% glycerol, 2% sodium dodecyl sulfate) containing 10 mg/ml dithiothreitol and prolonged for 15 min in the same buffer containing 25 mg/ml iodoacetamide. After equilibration, Immobiline DryStrips were transferred onto 11.5% polyacrylamide gels and run in the EttanDalt Six system (GE Healthcare Bio-Sciences Corp.) at 30 W/gel for 5 h at 20°C. The gels were scanned with appropriate wavelengths for excitation and emission using Ettan DIGE Primo (GE Healthcare Bio-Sciences Corp.). Relative quantification of spot intensities and statistical evaluation were carried out with ImageMaster 2D Platinum software (GE Healthcare Bio-Sciences Corp.). The experiments were performed in quadruplicates. The protein spots that were statisti-

Figure 1 Induction of apoptosis by a novel HDAC inhibitor NCH-51. (**a**) The growth inhibitory effects of NCH-51 and suberoylanilide hydroxamic acid (SAHA) on 13 lymphoid malignant cell lines. The cells were treated with either NCH-51 or SAHA (3 μM) for 24 or 72 h. Cell growth was estimated by 3-(4,5-dimethylthiazol-2-yl)-2,5-diphenyltetrazolium bromide (MTT) assay and gray-scale levels represent the growth inhibition rate (%) compared to untreated control. Each value indicates the mean IC_{50}. (**b**) Growth inhibitory effects of NCH-51 and SAHA on U266 cells and four control peripheral blood mononuclear cells (PBMCs). A multiple myeloma cell line U266 cells, and four healthy donor PBMCs were treated with indicated concentrations (0–30 μM) of NCH-51 (closed symbols) or SAHA (opened symbols) for 24 h. Cell growth was evaluated by MTT assay. The results are shown as the percentage cell growth compared to untreated control. These experiments were performed in triplicates and the mean values±s.d. are shown. *$P<0.05$; **$P<0.01$. (**c**) Induction of apoptosis by NCH-51. U266 cells were treated with the indicated concentrations (0–30 μM) of NCH-51 for 18 h, stained with fluorescein isothiocyanate-conjugated annexin V, and analyzed by flowcytometry. Annexin V-positive fraction indicates the cells undergoing apoptosis. (**d**) Activation of caspases and poly-ADP ribose polymerase (PARP) cleavage by NCH-51. U266 cells were treated with 3 μM of NCH-51 for 0–24 h. Whole cell extracts were prepared and subjected to immunoblots with the indicated antibodies. Positions of uncleaved (inactivated) and cleaved (activated) caspases and PARP proteins are indicated by arrows.

cally significant between untreated control and treated sample were selected.

Protein identification by mass spectrometry

For mass spectrometric analysis, 400 μg of unlabeled-protein extract was independently applied to 2D electrophoresis. The gel was stained with DeepPurple solution (GE Healthcare Bio-Sciences Corp.) according to the manufacturer's recommendation. The gel image was obtained by scanning with Ettan DIGE Primo and matched to those of analytical gels by using the ImageMaster 2D Platinum software. The spots of interest were picked out, and in-gel protein digestion was carried out with trypsin gold (Promega, Madison, WI, USA) as described.[26] Mass spectrometric analyses were performed by using a MALDI-TOF/TOF type mass spectrometer AB4700 (Applied Biosystems, Framingham, MA, USA). The proteins were identified through the online search using MASCOT database search engine.

Immunoblot analysis

The cell extracts obtained from cell cultures treated with or without HDACi were subjected to cell extract preparation as described above. The samples were applied to electrophoresis on a 10% polyacrylamide gel and transferred onto a nitrocellulose membrane. The membranes were incubated in TBS-T (10 mM Tris–HCl (pH, 8.0), 150 mM NaCl, 0.1% Tween) with 5% non-fat milk containing 1:1000 diluted primary antibodies against either caspase-9, -8, -7, -3, poly-ADP ribose polymerase (PARP) (Cell Signaling Technology, Danvers, MA, USA), peroxiredoxin 1 (Affinity Bioreagents, Golden, CO, USA), elongation factor-2 or α-tubulin (Santa Cruz, Santa Cruz, CA, USA). Membranes were then rinsed in TBS-T and further incubated with HRP-conjugated secondary antibody (GE Healthcare Bio-Sciences Corp.) in TBS-T with 5% non-fat milk. Each protein was detected by SuperSignal (PIERCE, Rockford, IL, USA).

Detection of ROS

ROS content was measured as described previously.[27] After treatment with HDACi, the cells were incubated with an oxidation-sensitive fluorescent probe 2′, 7′-dichlorofluorescein diacetate (H_2-DCFDA) (Molecular Probes Inc., Eugene, OR, USA) at a final concentration of 5 μM for 30 min. The cells were washed and resuspended in PBS, and then ROS amount was measured by flowcytometry.

Results

NCH-51 induces apoptosis greater than SAHA

We first evaluated the growth inhibitory effects of NCH-51 on a variety of lymphoid malignant cell lines (Figure 1a). A tentative result in a multiple myeloma cell line U266 cells is shown in Figure 1b. In most of the cell lines including U266 cells, NCH-51 exhibited a stronger growth inhibitory effect than SAHA at 3 μM for 24 h treatment, whereas prolonged incubation for 72 h did not show such a difference. It is noted that there was no significance in the growth inhibitory effect on four healthy donor PBMCs between NCH-51 and SAHA (IC_{50} values of both agents were higher than 30 μM), suggesting a cell-type specific cytotoxicity of NCH-51. We then analyzed the apoptosis and cell cycle distribution after the treatment with NCH-51 or SAHA. In the six cell lines (Jurkat, ED-40515(−), MEC2, U266, XG7 and ILKM-2), all of which showed a high susceptibility to NCH-51 (IC_{50}<3 μM), NCH-51 strongly induced apoptosis greater than SAHA after 24 h treatment as demonstrated by generation of sub-G_1 cells (Figure 1c and Table 1). In fact, when U266 cells were treated with NCH-51, cleaved forms of caspase-9, -8, -3 and PARP could be detected after 8 h, evidently at 16 h, although no activation of caspase-7 was detected (Figure 1d), suggesting that NCH-51 induces apoptosis through both extrinsic (type I) and intrinsic (type II) pathways[28] in the short-term treatment. On the other hand, cell cycle analysis revealed that NCH-51 increased the cell number at G_2/M-phase and reduced the number at G_1- or S-phase in most of the cell lines examined (Table 1, right column). No significant difference in the effects on cell cycle regulation was observed between NCH-51- and SAHA-treated cells. These observations suggest that the apoptosis-inducing activity might be attributable to the difference in the observed growth inhibitory effects between NCH-51 and SAHA.

NCH-51 regulates the expressions of antioxidant molecules at the protein level

To identify the target molecules regulated by NCH-51, we analyzed the RNA and protein expression profiles. cDNA microarray analysis using U266 cells showed that NCH-51 treatment upregulated the expression of *p21* and *p19* (Supplementary Table 1), confirming the previous reports by us[11] and others.[12–14] On the other hand, NCH-51 downregulated the gene expression of *CFLAR* (*c-FLIP*), *survivin* and *BCL2L2* (*bcl-w*), which act as antiapoptotic molecules. These results suggested that these genes were responsible for the growth inhibitory action of NCH-51, however, there was no notable difference in mRNA expression between NCH-51- and SAHA-treated cells. We then performed the proteome analysis. Whole cell extracts were prepared from U266 cells treated with or without NCH-51, and the protein samples were labeled with fluorescent dyes and applied to 2D electrophoresis (Figure 2a). By comparing the amounts of cellular proteins, we identified 14 proteins that varied relatively to NCH-51 treatment (Table 2). Ten proteins including nucleotide diphosphate kinase A (NDPKA), peroxiredoxin 1 and 2 (PRDX1, 2), glutathione *S*-transferase P1-1 (GSTP1-1), 14-3-3 zeta/delta, Cl^- intracellular channel proteins 1 and 4 (CLIC1, 4), proteasome subunit α3, protease activator 28 β subunit and Rho GDI α were upregulated, and four proteins including alanyl-tRNA synthetase (AARS), elongation factor-2 (EF-2), heat-shock 70 kDa protein 8 (HSPA8) and mitochondrial inner membrane protein, were downregulated after the treatment with NCH-51. Interestingly, some of these proteins upregulated by NCH-51 belong to a class of antioxidant molecules. It is noted that PRDX1 and PRDX2 were upregulated at both mRNA and protein levels, thus they are considered to be upregulated at the gene expression level, whereas most of the proteins were upregulated without induction at the gene expression level. In contrast, EF-2 and HSPA8 were downregulated at the protein level. The effects of NCH-51 and SAHA on the expression of EF-2 and PRDX1 were then verified. As shown in Figure 2b, EF-2 protein level was decreased either by NCH-51 or SAHA in the cell lines such as U266, ED-40515 (−) and XG7 cells that were highly susceptible to HDACi. EF-2 was decreased after 16 h treatment with these HDACi (data not shown). On the other hand, in the cell lines such as MEC2, Daudi and KM5 cells that were less sensitive to HDACi, EF-2 protein level was not significantly changed. PRDX1 protein level was upregulated by the treatment with either NCH-51 or SAHA in ED-40515 (−), U266, XG7 and MEC2 cells. SAHA seemed to upregulate PRDX1 more than NCH-51.

Table 1 The profiles of apoptosis and cell cycle distribution

Cell line	*HDAC inhibitor (μM)*	*Apoptotic cell[a] (%)*	*Cell cycle distribution[a](%)*			
			sub G_1	*G_1*	*S*	*G_2/M*
Jurkat	Untreated control	6.30	5.11	50.39	20.76	20.64
	SAHA					
	3 μM	13.45	28.56	9.15	12.97	46.22
	30 μM	28.97	32.39	7.06	18.10	40.83
	NCH-51					
	3 μM	19.27	42.66	8.05	10.04	36.28
	30 μM	35.45	42.69	7.64	14.41	32.21
MT-2	Untreated control	6.84	3.02	63.25	15.29	15.64
	SAHA					
	3 μM	8.23	9.41	49.04	11.70	26.36
	30 μM	8.75	10.35	62.95	6.15	13.96
	NCH-51					
	3 μM	8.45	3.26	62.21	16.34	16.53
	30 μM	8.62	5.38	71.64	8.35	12.22
ED-40515 (−)	Untreated control	6.44	8.40	46.82	23.30	19.67
	SAHA					
	3 μM	20.74	18.88	21.41	19.07	36.90
	30 μM	20.12	26.87	22.20	20.49	27.75
	NCH-51					
	3 μM	22.12	27.10	28.04	19.04	23.91
	30 μM	21.33	26.54	25.09	20.56	25.72
MEC2	Untreated control	3.20	5.66	60.06	19.96	12.16
	SAHA					
	3 μM	4.84	12.32	37.33	19.84	26.70
	30 μM	8.22	18.14	29.46	22.63	25.12
	NCH-51					
	3 μM	6.50	16.22	36.43	19.28	24.75
	30 μM	11.08	21.24	30.47	20.93	23.29
MO1043	Untreated control	4.14	0.89	54.88	20.75	17.87
	SAHA					
	3 μM	4.30	3.45	68.83	7.49	15.41
	30 μM	15.96	18.85	48.29	6.62	23.14
	NCH-51					
	3 μM	3.74	2.47	73.90	7.17	12.88
	30 μM	14.93	21.75	48.79	6.14	21.03
Daudi	Untreated control	1.62	1.62	52.02	22.77	19.55
	SAHA					
	3 μM	2.08	2.17	23.65	22.33	46.30
	30 μM	2.12	2.34	22.83	19.75	48.21
	NCH-51					
	3 μM	2.64	1.90	50.38	14.74	27.71
	30 μM	3.04	2.19	25.68	22.19	43.28
U266	Untreated control	6.17	6.30	67.42	10.99	13.02
	SAHA					
	3 μM	17.65	11.91	56.24	10.35	19.72
	30 μM	29.73	17.06	48.70	12.69	19.68
	NCH-51					
	3 μM	22.90	13.39	54.07	11.60	18.62
	30 μM	32.63	18.90	49.15	13.40	18.94
XG7	Untreated control	7.27	7.58	49.21	20.34	23.37
	SAHA					
	3 μM	8.74	8.50	50.40	8.33	28.32
	30 μM	9.43	15.38	34.23	15.10	28.21
	NCH-51					
	3 μM	11.47	10.00	49.32	8.62	28.62
	30 μM	13.13	17.87	35.44	14.67	27.93
KM5	Untreated control	4.24	2.91	42.15	27.85	23.43
	SAHA					
	3 μM	4.30	6.32	31.85	31.44	26.13
	30 μM	15.96	23.37	20.62	26.19	24.68
	NCH-51					
	3 μM	3.74	6.75	38.34	29.96	20.84
	30 μM	18.46	20.33	27.77	23.29	24.31

Table 1 (*Continued*)

Cell line	*HDAC inhibitor (μM)*	*Apoptotic cell[a] (%)*	*Cell cycle distribution[a](%)*			
			sub G_1	*G_1*	*S*	*G_2/M*
ILKM-2	Untreated control	7.35	4.07	58.61	13.05	22.89
	SAHA					
	3 μM	7.84	8.97	61.53	6.23	22.12
	30 μM	21.41	20.63	51.10	12.71	13.88
	NCH-51					
	3 μM	8.71	6.04	63.21	6.93	22.45
	30 μM	30.04	20.54	51.45	12.15	15.13

Abbreviations: HDAC, histone deacetylase; SAHA, suberoylanilide hydroxamic acid.
[a]Each value shows the average of 20 000 cells counted.

NCH-51 induces cytotoxic effect through the modulation of intracellular ROS

From the results of proteome analyses, NCH-51 appeared to promote the expression of antioxidant molecules, either at the transcriptional or post-transcriptional level, which prompted us to examine the effect of NCH-51 on the levels of ROS accumulation. Interestingly, the temporal profile of ROS amount in U266 cells treated with NCH-51 appeared to be in a concave shape indicating a gradual suppression of ROS accumulation within the initial 4 h and subsequent induction of ROS (Figure 3a), whereas the temporal profile with SAHA continuously declined over time. Similar trends were observed with other cell lines (data not shown). As summarized in Table 2, SAHA was more effective in reducing ROS than NCH-51, and the difference in ROS amount between NCH-51 and SAHA was most evident at 24 h, when the difference in growth inhibitory effect could be observed (Figure 1). These results suggested a possibility that dynamic state of ROS in each cell could be attributed to the growth inhibitory effect of HDACi. We thus examined whether NAC, a small-molecule antioxidant compound, could modulate the effect of NCH-51 (Figure 3b). Expectedly, when U266 cells were pretreated with NAC, the NCH-51-mediated cell growth inhibition was abolished. Similar effect was observed in SAHA-treated cells as much as in NCH-51-treated cells (data not shown). These results indicated that high amount of ROS might be necessary for the induction of NCH-51-mediated cytotoxicity.

Discussion

There have been accumulating reports of successful inhibition of cancer cell growth using small-molecule HDACi compounds.[1,7] Initial studies with SAHA indicated that the mode of action of HDACi might be through upregulating the transcriptionally repressed genes during carcinogenic processes by acetylating the repressive histones.[12–14] However, recent reports have demonstrated that HDACi compounds also exert anticancer effects through acetylation of non-histone substrates.[15–19] For example, HDAC6, a microtubule-associated deacetylase, was shown to be responsible for transportation of misfolded proteins to aggresome thus promoting protein degradation.[19,29] Thus, we have attempted to clarify the mechanism of anticancer effects of NCH-51 by examining both mRNA and protein levels.

In this study, we noticed that NCH-51 induced apoptosis in sensitive cell lines greater than SAHA (Figures 1 and 2a and Table 1). Analyses of mRNA expression levels in NCH-51- and SAHA-treated cells has revealed that transcriptional repression of antiapoptotic genes, such as *survivin*, *bcl-w* and *c-FLIP* and upregulation of cell cycle regulators, such as *p21* and *p19*, could be attributable to the induction of apoptosis and cell cycle arrest, respectively (Supplementary Table 1, 2 and Supplementary Figure 1), supporting the previous findings by others.[12–14] There was no difference in the mRNA expression level between NCH-51- and SAHA-treated samples (Supplementary Figure 1). We have confirmed no difference in inducing activity for acetylation of histone H4 between these two HDACi's (Supplementary Figure 2). These findings suggest that NCH-51 and SAHA similarly affect gene expression presumably through histone acetylation. We thus examined the effects of these compounds on protein expression profile to understand the difference between NCH-51 and SAHA at the post-transcriptional level.

Interestingly, our proteome analyses revealed the upregulation of some antioxidant molecules including PRDX1, PRDX2 and GSTP1-1 (Table 2 and Figure 2). In addition, previous reports indicated that some other proteins identified by the present proteome analysis (Table 2) could be activated by oxidative stress.[30–34] For example, NDPKA is reported to be activated by ROS and protected the cell from ROS-induced apoptosis.[30,31] CLIC1 protein contains a redox-active site and is activated during ROS-triggered apoptosis.[32,33] These findings suggested a possibility that NCH-51 might induce the cytotoxic effect by modulating the intracellular ROS content. In fact, pretreatment with NAC abolished the growth inhibitory effect of NCH-51 (Figure 3b). These results support the previous findings by others, which showed the ROS accumulation by HDACi.[14,34,35] However, in contrast to the previous reports, both NCH-51 and SAHA downregulated the ROS content after 24 h treatment in most of the cell lines tested except for KM5 cells, in which ROS was increased by the treatment with SAHA or NCH-51 (Table 3). These findings were reproducibly observed. Although we currently do not know the reason why there was a discrepancy between our study and others, we think the time-point and/or cell characteristics may be different between them. When temporal profiles of ROS accumulation were examined (Figure 3a), we found a typical bimodal kinetics of the intracellular ROS content after treatment with NCH-51; an initial downregulation and subsequent upregulation of ROS. On the other hand, SAHA did not follow the similar kinetics and the intracellular ROS level gradually and continuously decreased (Figure 3a). Therefore, it is possible that apparent differences in the ability of cell growth inhibition between NCH-51 and SAHA, may be explained through the different effects on the redox status of cells and induction of antioxidant proteins. Interestingly, our proteome/transcriptome analyses have revealed that the upregulation of antioxidant molecules occurred at either protein or mRNA levels: GSTP1-1 was upregulated by

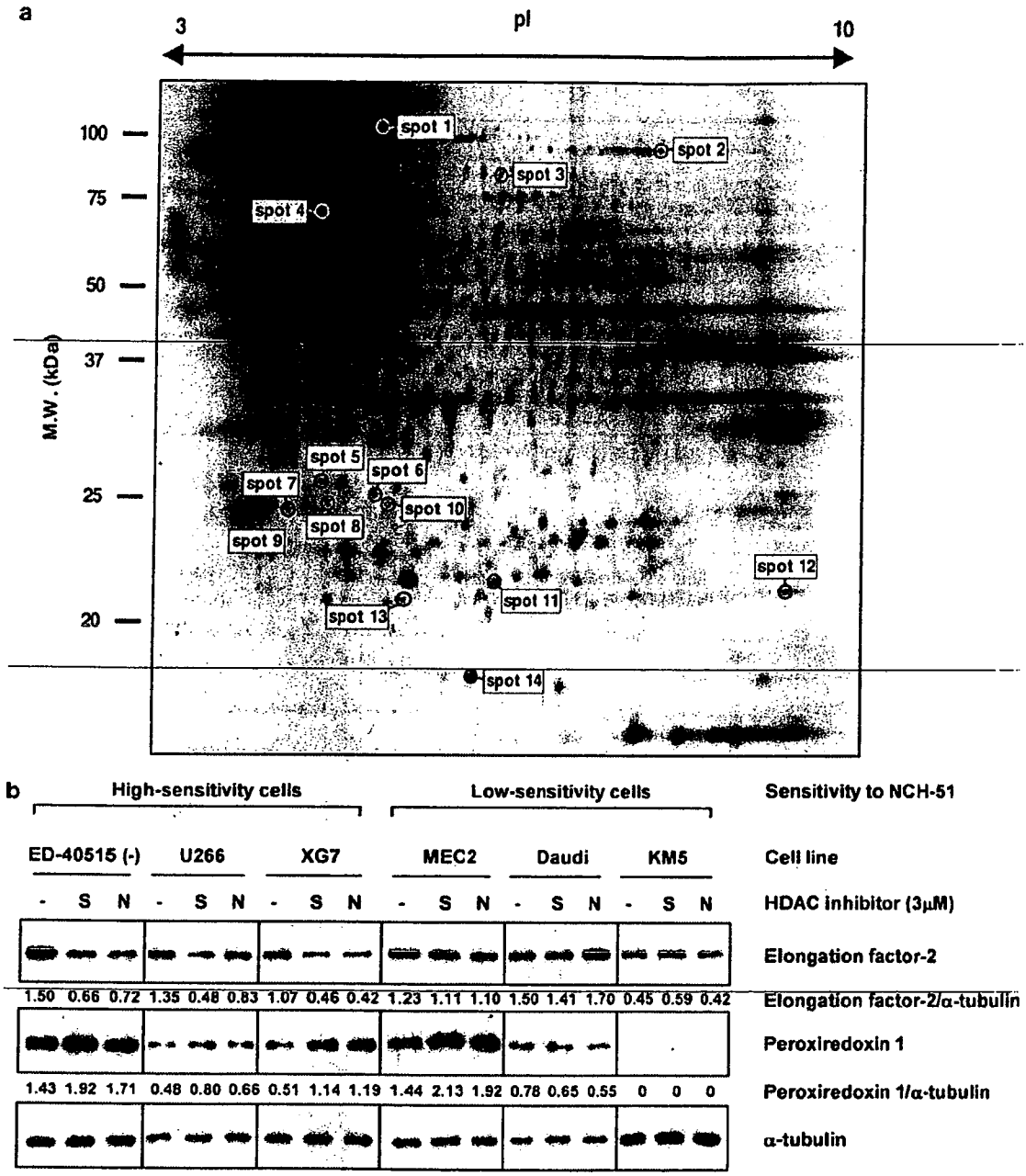

Figure 2 Proteome analysis of the effects of NCH-51. (a). 2D electrophoresis image of whole cell proteins prepared from U266 cells. After U266 cells were treated with or without 3 μM NCH-51 for 18 h, the whole cell extracts were prepared and applied to 2D electrophoresis in quadruplicates. Fourteen spots, whose relative amounts were either increased or decreased by the treatment with NCH-51 in all four gels, were indicated. Each spot number in the image corresponds to those in Table 2. MW, molecular weight (kDa). pI, isoelectric point. (b) Downregulation of elongation factor-2 (EF-2) and upregulation of peroxiredoxin 1 (PRDX1) by HDACi. The cells were treated with suberoylanilide hydroxamic acid (S) or NCH-51 (N) (3 μM) for 18 h. Whole cell extracts were prepared and subjected to immunoblots with the indicated antibodies. Each value means the ratio of the protein amount to α-tubulin (internal control).

NCH-51 only at the protein level, and PRDX1 and PRDX2 were upregulated primarily at the transcriptional level. These findings suggest that there may be two consequent antioxidative mechanisms by which HDACi modulate ROS accumulation: (i) the mRNA level, acting through induction of transcription of antioxidant molecules *de novo*, and (ii) the protein level, which was presumably caused by blocking the cellular protein transport/degradation pathway involving aggresome and proteasome. Importantly, we have observed that SAHA but not NCH-51 could induce acetylations of α-tubulin and HSP90 (Supplementary Figure 2), suggesting that SAHA might prolong the latter mechanism through blocking the degradation of antioxidant molecules. In fact, SAHA seemed to increase protein expression of PRDX1 greater than NCH-51 (Figure 2b). Since NCH-51 does not retain antioxidant molecules at the protein level, it induces the accumulation of ROS. Cellular levels of antioxidant molecules have been reported to be associated with the sensitivity to conventional anticancer agents.[36] Therefore,

Table 2 Upregulated/downregulated proteins after the treatment with NCH-51 in U266 cells

Spot no.	*Protein ID*	*Protein name*	*MW*	*pI*	*Protein ratio (T/C)*[a]	*mRNA ratio (T/C)*[a]
1	NP_001596	Alanyl-tRNA synthetase (AARS)	106734	5.31	0.80	0.74
2	NP_001952	Elongation factor-2 (EF-2)	95146	6.42	0.82	1.23
3	NP_006830	Mitochondrial inner membrane protein (IMMT)	83626	6.08	0.83	0.64
4	NP_006588	Heat-shock 70 kDa protein 8 (HSPA8)	70854	5.28	0.82	1.18
5	NP_001279	Cl^- intracellular channel protein 1 (CLIC1)	26775	5.09	1.34	0.67
6	NP_002809	Protease activator 28 β subunit (PA28β)	27213	5.44	1.54	1.03
7	NP_004300	Rho GDP-dissociation inhibitor 1 (Rho GDIα)	23193	5.02	1.42	0.92
8	NP_002779	Proteasome subunit α type3	28284	5.19	1.32	0.73
9	NP_663723	14-3-3 ζ/δ (PKC inhibitor protein 1)	28828	4.73	1.37	0.83
10	NP_039234	Cl intracellular channel protein 4 (CLIC4)	28754	5.45	1.38	0.86
11	NP_000843	Glutathione *S*-transferase P 1–1(GSTP1-1)	23210	5.44	1.38	0.98
12	NP_002565	Peroxiredoxin 1 (thioredoxin peroxidase 2) (PRDX1)	22096	8.27	1.30	1.4
13	NP_005800	Peroxiredoxin 2 (thioredoxin peroxidase 1) (PRDX2)	21747	5.67	1.30	1.35
14	NP_000260	Nucleoside disphosphate kinase A (NDPKA)	17138	5.83	1.50	1.04

[a]The results are indicated as the ratio of NCH-51-treated sample to untreated control (T/C).

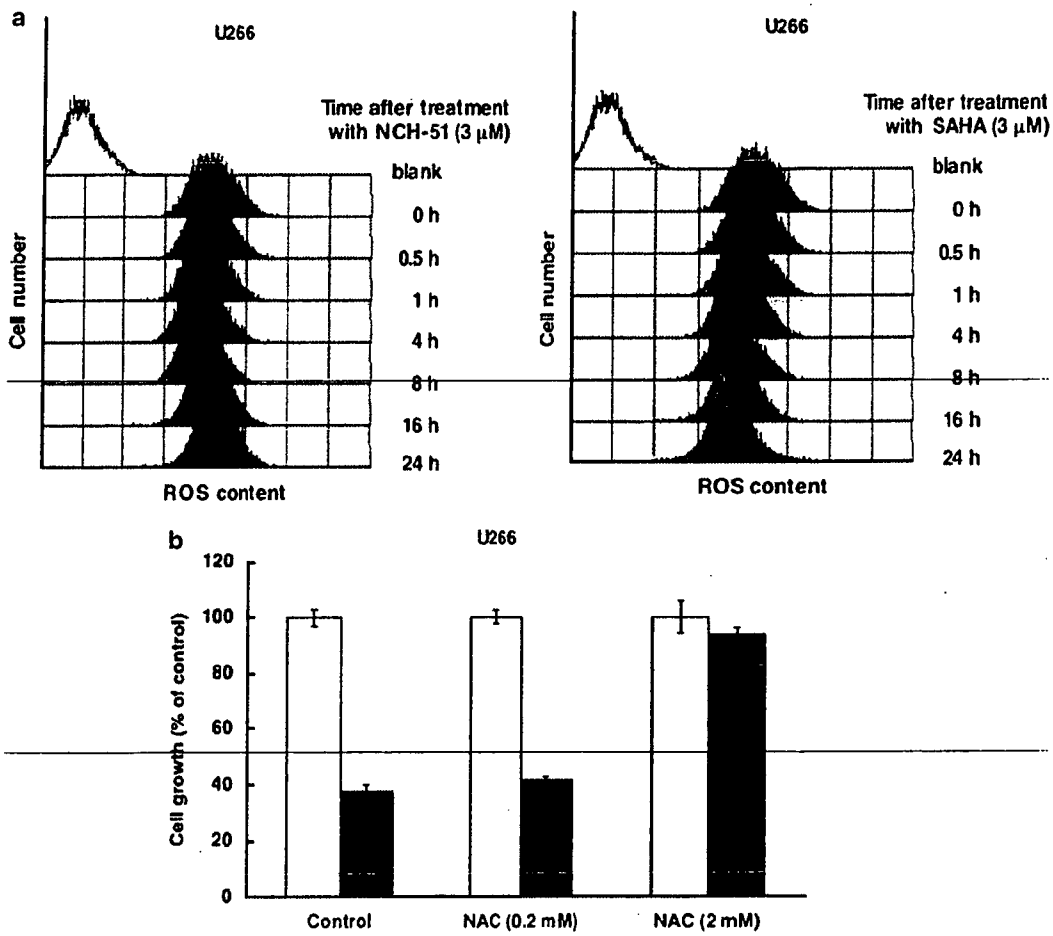

Figure 3 Effects of NCH-51 and suberoylanilide hydroxamic acid (SAHA) on reactive oxygen species (ROS) accumulation. (**a**) Time course of intracellular ROS after the treatment with HDACi. U266 cells were treated with NCH-51 or SAHA (3 μM) given the indicated time (0–24 h). After the treatment, H_2-DCFDA was added and further incubated for 30 min. ROS content was measured by flowcytometry. Blank, H_2-DCFDA-untreated control. (**b**) Effects of *N*-acetyl-L-cysteine (NAC) on the NCH-51-induced cell growth inhibition. U266 cells were treated with or without NCH-51 (3 μM) for 24 h in the presence or absence of NAC (0.2 or 2 mM). Cell growth was measured by 3-(4,5-dimethylthiazol-2-yl)-2,5-diphenyltetrazolium bromide assay. Open and closed bars indicate untreated and the NCH-51-treated cells. The results are shown as the percentage compared to untreated control. Experiments were done in triplicates and the mean values ± s.d. are shown.

NCH-51 can not only induce apoptosis through ROS accumulation, but also enhance the cytotoxicity of other agents in the combination treatment more efficiently than SAHA.

Our proteome analysis has also identified several proteins other than antioxidant molecules, including EF-2, AARS and HSPA8. We confirmed that EF-2 protein, a member of the GTP-

Table 3 ROS content and growth inhibitory effect after the treatment with HDAC inhibitor

Cell line	ROS content (% of control)[a]		Growth inhibition (% of control)[b]	
	NCH-51 (3 μM)	SAHA (3 μM)	NCH-51 (3 μM)	SAHA (3 μM)
Jurkat	86	47	63.5±0.8	37.7±2.5
MT-2	100	100	38.8±0.3	11.0±2.3
ED-40515 (−)	82	56	71.2±1.2	44.1±1.0
MEC2	59	46	41.3±1.1	3.5±2.8
MO1043	91	65	46.0±0.5	7.2±2.9
Daudi	74	54	25.6±1.8	15.1±3.0
U266	95	85	80.7±1.8	51.7±3.2
XG7	74	28	66.5±1.1	23.1±1.6
KM5	126	119	20.5±0.5	14.6±1.2
ILKM-2	94	94	85.5±0.2	81.3±1.1

Abbreviations: HDAC, histone deacetylase; ROS, reactive oxygen species; SAHA, suberoylanilide hydroxamic acid.
[a]Each value shows the average of 20 000 cells counted.
[b]Each value shows the mean±s.d.

binding translational elongation factor family,[37] was specifically decreased in high-sensitivity cell lines such as ED-40515 (−) and U266 cells (Figure 2b) after 16 h treatment (data not shown). However, gene expression of EF-2 was upregulated after the treatment with NCH-51 (Table 2). This discrepancy indicates a possibility that NCH-51 could induce rapid turnover of EF-2 protein followed by upregulation of RNA expression. Similar effects on EF-2 were also observed with SAHA (Figure 2b). Since EF-2 has been reported to be inactivated by ROS and lead to inhibition of translation,[38] it is suggested that locally induced ROS by HDACi might induce EF-2 inactivation and degradation presumably by direct oxidation. Although the mechanism by which EF-2 is downregulated by HDACi remains unclear, EF-2 may be used as a feasible surrogate marker to evaluate the susceptibility of HDACi. Similar to EF-2, AARS and HSPA8 were downregulated at the protein level. It is known that HSPA8 are involved in protein folding and transport.[39] Thus, these findings collectively suggest that NCH-51 might arrest protein synthesis and transportation.

In conclusion, our study demonstrates the therapeutic advantage of NCH-51 on growth inhibition of lymphoid malignant cells. Importantly, NCH-51 did not affect the cell growth of normal PBMCs with the effective concentrations on malignant cells (Figure 1b). In addition to its therapeutic efficacy and selectivity, NCH-51 has additional advantages in clinical use based on its pharmacological features. Therefore, NCH-51 could be a useful anticancer agent against lymphoid malignancies.

Acknowledgements

We thank Mr ME Cueno for language editing. This work is supported in part by grant-in-aids from the Ministry of Education, Culture, Sports, Science and Technology and the Ministry of Health, Labor and Welfare of Japan. TS is supported by a grant of Aichi Cancer Research Foundation and a grant of Oujinkai Foundation. HN, TS and NY are supported by a grant of Takeda Science Foundation.

References

1 Minucci S, Pelicci PG. Histone deacetylase inhibitors and the promise of epigenetic (and more) treatments for cancer. *Nat Rev Cancer* 2006; **6**: 38–51.
2 Strahl BD, Allis CD. The language of covalent histone modifications. *Nature* 2000; **403**: 41–45.
3 Turner BM. Cellular memory and the histone code. *Cell* 2002; **111**: 285–291.
4 Claus R, Lubbert M. Epigenetic targets in hematopoietic malignancies. *Oncogene* 2003; **22**: 6489–6496.
5 Fraga MF, Ballestar E, Villar-Garea A, Boix-Chornet M, Espada J, Schotta G *et al.* Loss of acetylation at Lys16 and trimethylation at Lys20 of histone H4 is a common hallmark of human cancer. *Nat Genet* 2005; **37**: 391–400.
6 Seligson DB, Horvath S, Shi T, Yu H, Tze S, Grunstein M *et al.* Global histone modification patterns predict risk of prostate cancer recurrence. *Nature* 2005; **435**: 1262–1266.
7 Kelly WK, Marks PA. Drug insight: histone deacetylase inhibitors–development of the new targeted anticancer agent suberoylanilide hydroxamic acid. *Nat Clin Pract Oncol* 2005; **2**: 150–157.
8 Kelly WK, O'Connor OA, Krug LM, Chiao JH, Heaney M, Curley T *et al.* Phase I study of an oral histone deacetylase inhibitor, suberoylanilide hydroxamic acid, in patients with advanced cancer. *J Clin Oncol* 2005; **23**: 3923–3931.
9 Ryan QC, Headlee D, Acharya M, Sparreboom A, Trepel JB, Ye J *et al.* Phase I and pharmacokinetic study of MS-275, a histone deacetylase inhibitor, in patients with advanced and refractory solid tumors or lymphoma. *J Clin Oncol* 2005; **23**: 3912–3922.
10 Golub LM, Lee HM, Ryan ME, Giannobile WV, Payne J, Sorsa T. Tetracyclines inhibit connective tissue breakdown by multiple non-antimicrobial mechanisms. *Adv Dent Res* 1998; **12**: 12–26.
11 Suzuki T, Nagano Y, Kouketsu A, Matsuura A, Maruyama S, Kurotaki M *et al.* Novel inhibitors of human histone deacetylases: design, synthesis, enzyme inhibition, and cancer cell growth inhibition of SAHA-based non-hydroxamates. *J Med Chem* 2005; **48**: 1019–1032.
12 Huang L, Sowa Y, Sakai T, Pardee AB. Activation of the p21WAF1/CIP1 promoter independent of p53 by the histone deacetylase inhibitor suberoylanilide hydroxamic acid (SAHA) through the Sp1 sites. *Oncogene* 2000; **19**: 5712–5719.
13 Richon VM, Sandhoff TW, Rifkind RA, Marks PA. Histone deacetylase inhibitor selectively induces p21WAF1 expression and gene-associated histone acetylation. *Proc Natl Acad Sci USA* 2000; **97**: 10014–10019.
14 Rosato RR, Almenara JA, Grant S. The histone deacetylase inhibitor MS-275 promotes differentiation or apoptosis in human leukemia cells through a process regulated by generation of reactive oxygen species and induction of p21CIP1/WAF1 1. *Cancer Res* 2003; **63**: 3637–3645.
15 Bali P, Pranpat M, Bradner J, Balasis M, Fiskus W, Guo F *et al.* Inhibition of histone deacetylase 6 acetylates and disrupts the chaperone function of heat shock protein 90: a novel basis for antileukemia activity of histone deacetylase inhibitors. *J Biol Chem* 2005; **280**: 26729–26734.
16 Hubbert C, Guardiola A, Shao R, Kawaguchi Y, Ito A, Nixon A *et al.* HDAC6 is a microtubule-associated deacetylase. *Nature* 2002; **417**: 455–458.

17 Insinga A, Monestiroli S, Ronzoni S, Carbone R, Pearson M, Pruneri G *et al.* Impairment of p53 acetylation, stability and function by an oncogenic transcription factor. *EMBO J* 2004; **23**: 1144–1154.
18 Chen L, Fischle W, Verdin E, Greene WC. Duration of nuclear NF-kappaB action regulated by reversible acetylation. *Science* 2001; **293**: 1653–1657.
19 Hideshima T, Bradner JE, Wong J, Chauhan D, Richardson P, Schreiber SL *et al.* Small-molecule inhibition of proteasome and aggresome function induces synergistic antitumor activity in multiple myeloma. *Proc Natl Acad Sci USA* 2005; **102**: 8567–8572.
20 Sanda T, Asamitsu K, Ogura H, Iida S, Utsunomiya A, Ueda R *et al.* Induction of cell death in adult T-cell leukemia cells by a novel IkappaB kinase inhibitor. *Leukemia* 2006; **20**: 590–598.
21 Uranishi M, Iida S, Sanda T, Ishida T, Tajima E, Ito M *et al.* Multiple myeloma oncogene 1 (MUM1)/interferon regulatory factor 4 (IRF4) upregulates monokine induced by interferon-gamma (MIG) gene expression in B-cell malignancy. *Leukemia* 2005; **19**: 1471–1478.
22 Pulvertaft JV. Cytology of Burkitt's tumour (African lymphoma). *Lancet* 1964; **39**: 238–240.
23 Klein E, Klein G, Nadkarni JS, Nadkarni JJ, Wigzell H, Clifford P. Surface IgM-kappa specificity on a Burkitt lymphoma cell *in vivo* and in derived culture lines. *Cancer Res* 1968; **28**: 1300–1310.
24 Suzuki A, Iida S, Kato-Uranishi M, Tajima E, Zhan F, Hanamura I *et al.* ARK5 is transcriptionally regulated by the Large-MAF family and mediates IGF-1-induced cell invasion in multiple myeloma: ARK5 as a new molecular determinant of malignant multiple myeloma. *Oncogene* 2005; **24**: 6936–6944.
25 Sanda T, Iida S, Ogura H, Asamitsu K, Murata T, Bacon KB *et al.* Growth inhibition of multiple myeloma cells by a novel IkappaB kinase inhibitor. *Clin Cancer Res* 2005; **11**: 1974–1982.
26 Seike M, Kondo T, Mori Y, Gemma A, Kudoh S, Sakamoto M *et al.* Proteomic analysis of intestinal epithelial cells expressing stabilized beta-catenin. *Cancer Res* 2003; **63**: 4641–4647.
27 Imai K, Nakata K, Kawai K, Hamano T, Mei N, Kasai H *et al.* Induction of OGG1 gene expression by HIV-1 Tat. *J Biol Chem* 2005; **280**: 26701–26713.
28 Opferman JT, Korsmeyer SJ. Apoptosis in the development and maintenance of the immune system. *Nat Immunol* 2003; **4**: 410–415.
29 Kawaguchi Y, Kovacs JJ, McLaurin A, Vance JM, Ito A, Yao TP. The deacetylase HDAC6 regulates aggresome formation and cell viability in response to misfolded protein stress. *Cell* 2003; **115**: 727–738.
30 Song EJ, Kim YS, Chung JY, Kim E, Chae SK, Lee KJ. Oxidative modification of nucleoside diphosphate kinase and its identification by matrix-assisted laser desorption/ionization time-of-flight mass spectrometry. *Biochemistry* 2000; **39**: 10090–10097.
31 Arnaud-Dabernat S, Masse K, Smani M, Peuchant E, Landry M, Bourbon PM *et al.* Nm23-M2/NDP kinase B induces endogenous c-myc and nm23-M1/NDP kinase A overexpression in BAF3 cells. Both NDP kinases protect the cells from oxidative stress-induced death. *Exp Cell Res* 2004; **301**: 293–304.
32 Harrop SJ, DeMaere MZ, Fairlie WD, Reztsova T, Valenzuela SM, Mazzanti M *et al.* Crystal structure of a soluble form of the intracellular chloride ion channel CLIC1 (NCC27) at 1.4-A resolution. *J Biol Chem* 2001; **276**: 44993–45000.
33 Shimizu T, Numata T, Okada Y. A role of reactive oxygen species in apoptotic activation of volume-sensitive Cl(−) channel. *Proc Natl Acad Sci USA* 2004; **101**: 6770–6773.
34 Ruefli AA, Ausserlechner MJ, Bernhard D, Sutton VR, Tainton KM, Kofler R *et al.* The histone deacetylase inhibitor and chemotherapeutic agent suberoylanilide hydroxamic acid (SAHA) induces a cell-death pathway characterized by cleavage of Bid and production of reactive oxygen species. *Proc Natl Acad Sci USA* 2001; **98**: 10833–10838.
35 Ungerstedt JS, Sowa Y, Xu WS, Shao Y, Dokmanovic M, Perez G *et al.* Role of thioredoxin in the response of normal and transformed cells to histone deacetylase inhibitors. *Proc Natl Acad Sci USA* 2005; **102**: 673–678.
36 Yokomizo A, Ono M, Nanri H, Makino Y, Ohga T, Wada M *et al.* Cellular levels of thioredoxin associated with drug sensitivity to cisplatin, mitomycin C, doxorubicin, and etoposide. *Cancer Res* 1995; **55**: 4293–4296.
37 Ryazanov AG, Shestakova EA, Natapov PG. Phosphorylation of elongation factor 2 by EF-2 kinase affects rate of translation. *Nature* 1988; **334**: 170–173.
38 Patel J, McLeod LE, Vries RG, Flynn A, Wang X, Proud CG. Cellular stresses profoundly inhibit protein synthesis and modulate the states of phosphorylation of multiple translation factors. *Eur J Biochem* 2002; **269**: 3076–3085.
39 Young JC, Agashe VR, Siegers K, Hartl FU. Pathways of chaperone-mediated protein folding in the cytosol. *Nat Rev Mol Cell Biol* 2004; **5**: 781–791.

Supplementary Information accompanies the paper on the Leukemia website (http://www.nature.com/leu)

Journal of Cellular Physiology

Granulocyte Colony-Stimulating Factor Promotes the Translocation of Protein Kinase Cι in Neutrophilic Differentiation Cells

TOSHIE KANAYASU-TOYODA,[1] TAKAYOSHI SUZUKI,[1] TADASHI OSHIZAWA,[1] ERIKO UCHIDA,[2] TAKAO HAYAKAWA,[2] AND TERUHIDE YAMAGUCHI[1]*

[1]*Division of Cellular and Gene Therapy Products, National Institute of Health Sciences, Tokyo, Japan*

[2]*National Institute of Health Sciences, Tokyo, Japan*

Previously, we suggested that the phosphatidylinositol 3-kinase (PI3K)-p70 S6 kinase (p70 S6K) pathway plays an important role in granulocyte colony-stimulating factor (G-CSF)-dependent enhancement of the neutrophilic differentiation and proliferation of HL-60 cells. While atypical protein kinase C (PKC) has been reported to be a regulator of p70 S6K, abundant expression of PKCι was observed in myeloid and lymphoid cells. Therefore, we analyzed the participation of PKCι in G-CSF-dependent proliferation. The maximum stimulation of PKCι was observed from 15 to 30 min after the addition of G-CSF. From 5 to 15 min into this lag time, PKCι was found to translocate from the nucleus to the membrane. At 30 min it re-translocated to the cytosol. This dynamic translocation of PKCι was also observed in G-CSF-stimulated myeloperoxidase-positive cells differentiated from cord blood cells. Small interfering RNA for PKCι inhibited G-CSF-induced proliferation and the promotion of neutrophilic differentiation of HL-60 cells. These data indicate that the G-CSF-induced dynamic translocation and activation processes of PKCι are important to neutrophilic proliferation.

J. Cell. Physiol. 211: 189–196, 2007.

Hematopoietic cell differentiation is regulated by a complex network of growth and differentiation factors (Tenen et al., 1997; Ward et al., 2000). Granulocyte colony-stimulating factor (G-CSF) and its receptors are pivotal to the differentiation of myeloid precursors into mature granulocytes. In previous studies (Kanayasu-Toyoda et al., 2002) on the neutrophilic differentiation of HL-60 cells treated with either dimethyl sulfoxide (DMSO) or retinoic acid (RA), heterogeneous transferrin receptor (Trf-R) populations—transferrin receptor-positive ($Trf\text{-}R^+$) cells and transferrin receptor-negative ($Trf\text{-}R^-$) cells—appeared 2 days after the addition of DMSO or RA. The $Trf\text{-}R^+$ cells were proliferative-type cells that had higher enzyme activity of phosphatidylinositol 3-kinase (PI3K) and protein 70 S6 kinase (p70 S6K), whereas the $Trf\text{-}R^-$ cells were differentiation-type cells of which Tyr705 in STAT3 was much more phosphorylated by G-CSF. Inhibition of either PI3K by wortmannin or p70 S6K by rapamycin was found to eliminate the difference in differentiation and proliferation abilities between $Trf\text{-}R^+$ and $Trf\text{-}R^-$ cells in the presence of G-CSF (Kanayasu-Toyoda et al., 2002). From these results, we concluded that proteins PI3K and p70 S6K play important roles in the growth of HL-60 cells and negatively regulate neutrophilic differentiation. On the other hand, the maximum kinase activity of PI3K was observed at 5 min after the addition of G-CSF (Kanayasu-Toyoda et al., 2002) and that of p70 S6K was observed between 30 and 60 min after, indicating a lag time between PI3K and p70 S6K activation. It is conceivable that any signal molecule(s) must transduce the G-CSF signal during the time lag between PI3K and p70 S6K. Chung et al. (1994) also showed a lag time between PI3K and p70 S6K activation on HepG2 cells stimulated by platelet-derived growth factor (PDGF), suggesting that some signaling molecules also may transduce between PI3K and p70S6K.

Protein kinase C (PKC) is a family of Ser/Thr kinases involved in the signal transduction pathways that are triggered by numerous extracellular and intracellular stimuli. The PKC family has been shown to play an essential role in cellular functions, including mitogenic signaling, cytoskeleton rearrangement, glucose metabolism, differentiation, and the regulation of cell survival and apoptosis. Eleven different members of the PKC family have been identified so far. Based on their structural similarities and cofactor requirements, they have been grouped into three subfamilies: (1) the classical or conventional PKCs (cPKCα, β_1, β_2, and γ), activated by Ca^{2+}, diacylglycerol, and phosphatidyl-serine; (2) the novel PKCs (nPKCδ, ε, η, and θ), which are independent of Ca^{2+} but still responsive to diacylglycerol; and (3) the atypical PKCs (aPKCζ and ι/λ), where PKCλ is the homologue of human PKCι. Atypical PKCs differ significantly from all other PKC family

Abbreviations: DMSO, dimethyl sulfoxide; fMLP-R, formyl-Met-Leu-Phe receptor; RA, retinoic acid; G-CSF, granulocyte colony-stimulating factor; Trf-R, transferrin receptor; BSA, bovine serum albumin; FITC, fluorescein isothiocyanate; PBS, phosphate-buffered saline; PKC, protein kinase C; PI3K, phosphatidylinositol 3-kinase; p70 S6K, protein 70 S6 kinase; SDS-PAGE, sodium dodecyl sulfate-polyacrylamide gel electrophoresis; siRNA, small interfering RNA; PMN, polymorphonuclear leukocyte.

Contract grant sponsor: Ministry of Health, Labor, and Welfare of Japan.

Contract grant sponsor: Ministry of Education, Culture, Sports, Science, and Technology of Japan.

*Correspondence to: Teruhide Yamaguchi, Division of Cellular and Gene Therapy Products, National Institute of Health Sciences, 1-18-1, Kamiyoga, Setagaya-ku, Tokyo 158-8501, Japan.
E-mail: yamaguch@nihs.go.jp

Received 31 May 2006; Accepted 22 September 2006

Published online in Wiley InterScience (www.interscience.wiley.com.), 28 November 2006.
DOI: 10.1002/jcp.20930

members in their regulatory domains, in that they lack both the calcium-binding domain and one of the two zinc finger motifs required for diacylglycerol binding (Liu and Heckman, 1998). Romanelli et al. (1999) reported that p70 S6K is regulated by PKCζ and participates in a PI3K-regulated signaling complex. On the other hand, Selbie et al. (1993) reported that the tissue distribution of PKCζ is different from that of PKCι/λ, and that PKCι/λ appears to be widely expressed. If the p70 S6K could be activated by aPKC, the regulation of p70 S6K activation would seem to depend on the tissue-specific expression of PKCι and/or PKCζ. In neutrophilic lineage cells, the question is which aPKC participates in the regulation of p70 S6K on G-CSF signaling.

In this study, we show that G-CSF activated PKCι, promoting its translocation from the nucleus to the cell surface membrane and subsequently to the cytosol in DMSO-treated HL-60 cells. We also show the translocation of PKCι using myeloperoxidase-positive neutrophilic lineage differentiated from cord blood, which is a rich source of immature myeloid cells (Fritsch et al., 1993; Rappold et al., 1997; Huang et al., 1999; Debili et al., 2001; Hao et al., 2001). We concluded that PKCι translocation and activation by G-CSF are needed for neutrophilic proliferation.

Materials and Methods

Reagents

Anti-p70 S6K polyclonal antibody was obtained from Santa Cruz Biotechnology (Santa Cruz, CA). Anti-PKCι polyclonal antibody and monoclonal antibody were purchased from Santa Cruz Biotechnology and from Transduction Laboratories (Lexington, KY), respectively. Anti-PKCζ polyclonal antibody was purchased from Cell Signaling Technology (Beverly, MA). Anti-myeloperoxidase antibody was purchased from Serotec Ltd. (Oxford, UK). GF 109203X, and Gö 6983 were obtained from Calbiochem-Novabiochem (San Diego, CA). Wortmannin was obtained from Sigma Chemical (St. Louis, MO). Anti-Histon-H1 antibody, anti-Fcγ receptor IIa (CD32) antibody, and anti-lactate dehydrogenase antibody were from Upstate Cell Signaling Solutions (Lake Placid, NY), Lab Vision Corp. (Fremont, CA), and Chemicon International, Inc. (Temecula, CA), respectively.

Cell culture

HL-60, Jurkut, K562, U937, and THP-1 cells were kindly supplied by the Japanese Collection of Research Bioresources Cell Bank (Osaka, Japan). Cells were maintained in RPMI 1640 medium containing 10% heat-inactivated FBS and 30 mg/L kanamycin sulfate at 37°C in moisturized air containing 5% CO_2. The HL-60 cells, which were at a density of 2.5×10^5 cells/ml, were differentiated by 1.25% DMSO. Two days after the addition of DMSO, the G-CSF-induced signal transduction was analyzed using either magnetically sorted cells or non-sorted cells.

Magnetic cell sorting

To prepare Trf-R^- and Trf-R^+ cells, magnetic cell sorting was performed as previously reported (Kanayasu-Toyoda et al., 2002), using an automatic cell sorter (AUTO MACS; Miltenyi Biotec, Bergisch Gladbach, Germany). After cell sorting, both cell types were used for Western blotting and PKCι enzyme activity analyses.

Preparation of cell lysates and immunoblotting

For analysis of PKCι and PKCζ expression, a PVDF membrane blotted with 50 μg of various tissues per lane was purchased from BioChain Institute (Hayward, CA). Both a polymorphonuclear leukocytes (PMNs) fraction and a fraction containing lymphocytes and monocytes were isolated by centrifugation (400g, 25 min) using a Mono-poly resolving medium (Dai-Nippon Pharmaceutical, Osaka, Japan) from human whole blood, which was obtained from a healthy volunteer with informed consent. T-lymphocytes were further isolated from the mixture fraction using the Pan T Cell Isolation Kit (Miltenyi Biotec) according to the manufacturer's protocol. T-lymphocytes, PMNs, HL-60 cells, Jurkut cells, K562 cells, and U937 cells (1×10^7) were collected and lysed in lysis buffer containing 1% Triton X-100, 10 mM K_2HPO_4/KH_2PO_4 (pH 7.5), 1 mM EDTA, 5 mM EGTA, 10 mM $MgCl_2$, and 50 mM β-glycerophosphate, along with 1/100 (v/v) protease inhibitor cocktail (Sigma Chemical) and 1/100 (v/v) phosphatase inhibitor cocktail (Sigma Chemical). The cellular lysate of 10^6 cells per lane was subjected to Western blotting analysis. Human cord blood was kindly supplied from the Metro Tokyo Red Cross Cord Blood Bank (Tokyo, Japan) with informed consent. Mononuclear cells, isolated with the Lymphoprep™ Tube (Axis-Shield PoC AS, Oslo, Norway), were cultured in RPMI 1640 medium containing 10% FBS in the presence of G-CSF for 3 days. Cultured cells were collected, and the cell lysate was subjected to Western blotting analysis.

A fraction of the plasma membrane, cytosol, and nucleus of the DMSO-treated HL-60 cells was prepared by differential centrifugation after the addition of G-CSF, as described previously (Yamaguchi et al., 1999). After the cells that had been suspended in 250 mM sucrose/10 mM Tris-HCl (pH 7.4) containing 1/100 (v/v) protease inhibitor cocktail (Sigma Chemical) were gently disrupted by freezing and thawing, they were centrifuged at 800g, 4°C for 10 min. The precipitation was suspended in 10 mM Tris-HCl (pH 6.7) supplemented with 1% SDS. It was then digested by benzon nuclease at 4°C for 1 h and used as a sample of the nuclear fraction. After the post-nucleus supernatant was re-centrifuged at 100,000 rpm (452,000g) at a temperature of 4°C for 40 min, the precipitate was used as a crude membrane fraction and the supernatant as a cytosol fraction. Western blotting analysis was then performed as described previously (Kanayasu-Toyoda et al., 2002). The bands that appeared on x-ray films were scanned, and the density of each band was quantitated by Scion Image (Scion, Frederick, MD) using the data from three separate experiments.

Kinase assay

The activity of PKCι was determined by phosphorous incorporation into the fluorescence-labeled pseudosubstrate (Pierce Biotechnology, Rockford, IL). The cell lysates were prepared as described above and immunoprecipitated with the anti-PKCι antibody. Kinase activity was measured according to the manufacturer's protocol. In the analysis of inhibitors effects, cells were pretreated with a PI3K inhibitor, wortmannin (100 nM), or PKC inhibitors, GF109207X (10 μM) and Gö6983 (10 μM) for 30 min, and then stimulated by G-CSF for 15 min.

Observation of confocal laser-scanning microscopy

Upon the addition of G-CSF, PKCι localization in the DMSO-treated HL-60 cells for 2 days was examined by confocal laser-activated microscopy (LSM 510, Carl Zeiss, Oberkochen, Germany). The cells were treated with 50 ng/ml G-CSF for the indicated periods and then fixed with an equal volume of 4.0% paraformaldehyde in PBS(−). After treatment with ethanol, the fixed cells were labeled with anti-PKCι antibody and with secondary antibody conjugated with horseradish peroxidase. They were then visualized with TSA™ Fluorescence Systems (PerkinElmer, Boston, MA).

Mononuclear cells prepared from cord blood cells were cultured in RPMI 1640 medium containing 10% FBS in the presence of G-CSF for 7 days. Then, for serum and G-CSF starvation, cells were cultured in RPMI 1640 medium containing 1% BSA for 11 h. After stimulation by 50 ng/ml G-CSF, the cells were fixed, stained with both anti-PKCι polyclonal antibody and anti-myeloperoxidase monoclonal antibody, and finally visualized with rhodamine-conjugated anti-rabbit IgG and FITC-conjugated anti-mouse IgG, respectively.

RNA interference

Two pairs of siRNAs were chemically synthesized: annealed (Dharmacon RNA Technologies, Lafayette, CO) and transfected into HL-60 cells using Nucleofector™ (Amaxa, Cologne, Germany). The sequences of sense siRNAs were as follows: PKCι, GAAGAAGCCUUUAGACUUUTA; p70 S6K, GCAAGGAGUCUAUCCAUGAUU. As a control, the sequence ACUCUAUCGCCAGCGUGACUU was used. Forty-eight hours after treatment with siRNA, the cells were lysed for Western blot analysis. For proliferation and differentiation assay, cells were transfected with siRNA on the first day, treated with DMSO on the second day, and supplemented with G-CSF on the third day. After cells were subsequently cultured for 5 days, cell numbers and formyl-Met-Leu-Phe receptor (fMLP-R) expression were determined.

fMLP-R expression

The differentiated cells were collected and incubated with FITC-conjugated fMLP; then, labeled cells were subjected to flow cytometric analysis (FACSCalibur, Becton Dickinson, Franklin Lakes, NJ).

Statistical analysis

Statistical analysis was performed using unpaired Student's *t*-test. Values of $P < 0.05$ were considered to indicate statistical significance. Each experiment was repeated at least three times and representative data were indicated.

Results

The distribution of atypical PKC in various tissues and cells

Previously, we reported that the PI3K-p70 S6K-cMyc pathway plays an important role in the G-CSF-induced proliferation of DMSO-treated HL-60 cells, not only by enhancing the activity of both PI3K and p70 S6K but also by inducing the c-Myc protein (Kanayasu-Toyoda et al., 2002, 2003). We also reported that G-CSF did not stimulate Erk1, Erk2, or 4E-binding protein 1. The maximum kinase activity of PI3K was observed 5 min after the addition of G-CSF, and that of p70 S6K was observed between 30 and 60 min after. It is conceivable that any signal molecule(s) must transduce the G-CSF signal during the time lag between PI3K and p70 S6K. Romanelli et al. (1999) suggested that the activation of p70 S6K is regulated by PKCξ and participates in the PI3K-regulated signaling complex. To examine the role of atypical PKC in the G-CSF-dependent activation and the relationship between atypical PKC and p70 S6K, the protein expression of PKCζ and PKCι in various human tissues and cells was analyzed by Western blotting. As shown in Figure 1A, both of the atypical PKCs were markedly expressed in lung and kidney but were weakly expressed in spleen, stomach, and placenta. In brain, cervix, and uterus, the expression of only PKCι was observed. Selbie et al. (1993) have reported observing the expression of PKCζ not in protein levels but in RNA levels, in the kidney, brain, lung, and testis, and that of PKCι in the kidney, brain, and lung. In this study, the protein expression of PKCι in the kidney, brain, and lung was consistent with the RNA expression of PKCι. Despite the strong expression of PKCζ RNA in brain (Selbie et al., 1993), PKCζ protein was scarcely observed. Although PKCι proteins were scarcely expressed in neutrophils and T-lymphocytes in peripheral blood, they were abundantly expressed in immature blood cell lines, that is, Jurkut, K562, U937, and HL-60 cells (Fig. 1B), in contrast with the very low expression of PKCζ proteins. In mononuclear cells isolated from umbilical cord blood, which contains large numbers of immature myeloid cells and has a high proliferation ability, the expression of PKCι proteins was also observed. Since Nguyen and Dessauer (2005) have reported observing abundant PKCζ proteins in THP-1 cells, as a positive control for PKCζ, we also performed a Western blot of THP-1 cells (Fig. 1B, right part). While PKCι was markedly expressed in both THP-1 and HL-60 cells, PKCζ was observed only in THP-1 cells.

These data suggested that PKCζ and PKCι were distributed differently in various tissues and cells, and that mainly PKCι proteins were expressed in proliferating blood cells.

Stimulation of PKCι activity by G-CSF

Among the 11 different members of the PKC family, the aPKCs (ζ and ι/λ) have been reported to activate p70 S6K activity and to be regulated by PI3K (Akimoto et al., 1998; Romanelli et al., 1999). As shown in Figure 1, although the PKCζ proteins were not detected by Western blotting in HL-60 cells or mononuclear cells isolated from cord blood cells, it is possible that PKCι could functionally regulate p70 S6K as an upstream

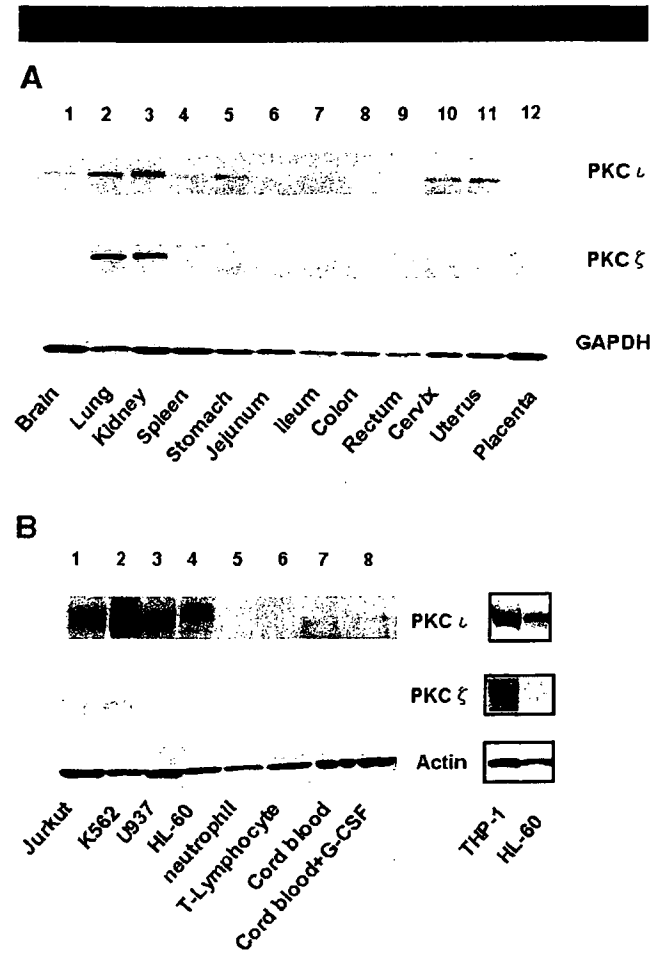

Fig. 1. Different distributions of PKCζ and PKCι. The protein expression of PKCι appears in the upper part and that of PKCζ in the middle part in various tissues and cells. A: 1, brain; 2, lung; 3, kidney, 4, spleen; 5, stomach; 6, jejunum; 7, ileum; 8, colon; 9, rectum; 10, cervix; 11, uterus; 12, placenta. Anti-GAPDH blot is a control for various tissues. B: 1, jurkut cells; 2, K562 cells; 3, U937 cells; 4, HL-60 cells; 5, neutrophils; 6, T-lymphocytes; 7, mononuclear cells from cord blood in the absence of G-CSF; 8, mononuclear cells from cord blood in the presence of G-CSF. Anti-actin blot is a control. The right part shows immunoblots of PKCι, PKCζ, and actin of THP-1 cells as a positive control for PKCζ. The cell numbers of THP-1 and HL-60 cells were adjusted in relation to other cells on the left parts.

regulator in these cells. Therefore, we focused on the role of PKCι as the possible upstream regulator of p70 S6K in neutrophil lineage cells. First, we compared the expression of PKCι in both Trf-R^+ and Trf-R^- cells. PKCι proteins were expressed more abundantly in Trf-R^+ cells than in Trf-R^- cells (Fig. 2A, middle part), as with the p70 S6K proteins. A time course study of PKCι activity upon the addition of G-CSF revealed the maximum stimulation at 15 min, lasting until 30 min. The G-CSF-dependent activation of PKCι was inhibited by the PKC inhibitors wortmannin, GF 109203X, and Gő 6983. Considering the marked inhibitory effect of wortmannin on PKCι and evidence that the maximum stimulation of PI3K was observed at 5 min after the addition of G-CSF, PI3K was determined to be the upstream regulator of PKCι in the G-CSF signal transduction of HL-60 cells. The basal activity of PKCι in Trf-R^+ cells was higher than that in Trf-R^- cells, and G-CSF was more augmented. In Trf-R^- cells, PKCι activity was scarcely stimulated by G-CSF. This tendency of PKCι to be activated by G-CSF was similar to that of PI3K (Kanayasu-Toyoda et al., 2002).

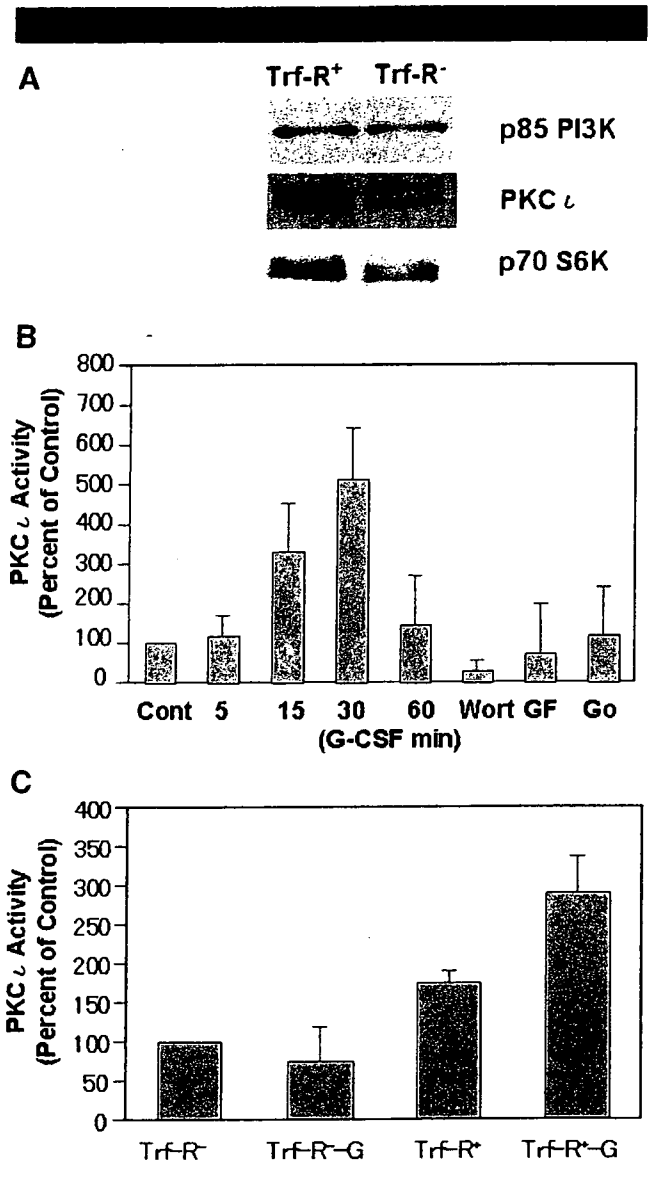

Fig. 2. Expression of PKCι in Trf-R$^+$ and Trf-R$^-$ cells and effects of G-CSF on PKCι activity. A: The expression of PKCι in Trf-R$^+$ and Trf-R$^-$ cells was subjected to Western blot analysis after magnetic cell sorting. B: The G-CSF-dependent PKCι activation of the DMSO-treated HL-60 cells was measured. The x-axis represents the time lapse (min) after the G-CSF stimulation and the y-axis percent of control that was not stimulated by G-CSF. Columns and bars represent the mean ± SD, using data from three separate experiments. Wort: wortmannin (100 nM), GF: GF109207X (10 μM), Gö: Gö6983 (10 μM). Cells were pretreated with each inhibitor and then stimulated by G-CSF for 15 min. C: The PKCι activity in the Trf-R$^+$ and Trf-R$^-$ cells 30 min after the addition of G-CSF. The y-axis represents the percentage of control that was non-stimulated Trf-R$^-$ cells. Columns and bars represent the mean ± SD, using data from three separate experiments.

Effects of G-CSF on PKCι translocation

Muscella et al. (2003) demonstrated that the translocation of PKCζ from the cytosol to the nucleus or membrane is required for c-Fos synthesis induced by angiotensin II in MCF-7 cells. It was also reported that high glucose induced the translocation of PKCι (Chuang et al., 2003). These results suggest that the translocation of aPKC plays an important role in its signaling. To clarify the translocation of PKCι, immuno-histochemical staining (Fig. 3) and biochemical fractionation (Fig. 4) in DMSO-induced HL-60 cells were performed after the addition of G-CSF. In a non-stimulated condition, PKCι in the HL-60 cells treated with DMSO for 2 days (Fig. 3, control) was detected mainly in the nucleus. Analysis of Western blotting (Fig. 4, left parts) and quantification of the bands (Fig. 4, right columns) also revealed that PKCι was localized and observed mainly in the nuclear fraction (Fig. 4A). During the 5–15 min period after the addition of G-CSF, PKCι was found to translocate (Figs. 3 and 4B) into the membrane fraction, after which it re-translocated into the cytosol fraction (Fig. 4C). In the presence of wortmannin, the G-CSF-induced translocation of PKCι into the plasma membrane failed, but PKCι was found to localize in the cytosolic fraction (Figs. 3 and 4B). Myeloperoxidase is thought to be expressed in stage from promyelocytes to mature neutrophils (Manz et al., 2002). In human cord blood cells (Fig. 3), PKCι in the cells co-stained with anti-myeloperoxidase antibody was also localized in the nucleus after serum depletion (Fig. 3B top parts). Ten minutes after the addition of G-CSF, PKCι was found to translocate into the membrane, and then into the cytosol at 30 min after the addition of G-CSF. In the presence of wortmannin, the G-CSF-induced translocation of PKCι into the plasma membrane failed but PKCι was found to localize in the cytosol. This suggested that the dynamic translocation of PKCι induced by G-CSF is a universal phenomenon in neutrophilic lineage cells. Taken together, these data support the possibility that PI3K plays not only an important role upstream of PKCι but also triggers the translocation from nucleus to membrane upon the addition of G-CSF.

In order to assess the purity of each cellular fraction, antibodies against specific markers were blotted. As specific markers, Histon-H1, Fcγ receptor IIa (CD32), and lactate dehydrogenase (LDH) were used for the nuclear, membrane, and cytosolic fractions, respectively. The purities of the nuclear, membrane, and cytosolic fractions were 82.0, 78.5, and 72.2%, respectively (Fig. 4D).

Effects of siRNA for PKCι on proliferation and differentiation

To determine the role of PKCι in neutrophilic proliferation and differentiation, PKCι was knocked down by siRNA. When the protein level of PKCι was specifically downregulated by siRNA for PKCι (Fig. 5A), G-CSF failed to enhance proliferation of the cells during 5 days' cultivation (Fig. 5B). The effect of siRNA for PKCι on neutrophilic differentiation in terms of fMLP-R expression was also determined. As shown in Figure 5C, fMLP-R expression was promoted by siRNA for PKCι in either the presence (lower part) or absence (upper part) of G-CSF. These data indicate that PKCι positively regulates G-CSF-induced proliferation and negatively regulates the differentiation of DMSO-treated HL-60 cells.

Discussion

We previously reported that PI3K/p70 S6K plays an important role in the regulation of the neutrophilic differentiation and proliferation of HL-60 cells. Akimoto et al. (1998) and Romanelli et al. (1999) reported that p70 S6K is regulated by aPKC and aPKCλ/PKCζ, respectively. At first, we showed that the distribution of PKCζ and PKCι proteins in various human tissues and cells was not similar (Fig. 1A), and that PKCι are more abundantly expressed in proliferating blood cells: Jurkut, K562, U937, and HL-60 cells (Fig. 1B). Moreover, PKCι proteins were also observed in cultured mononuclear cells of cord blood, in which the myeloid progenitors were enriched in the presence or absence of G-CSF (Fig. 1B). The myeloperoxidase-positive cells as neutrophilic lineage cells, a myeloid marker, were also stained with the antibody of PKCι (Fig. 3B). Although PKCζ proteins are barely detected in

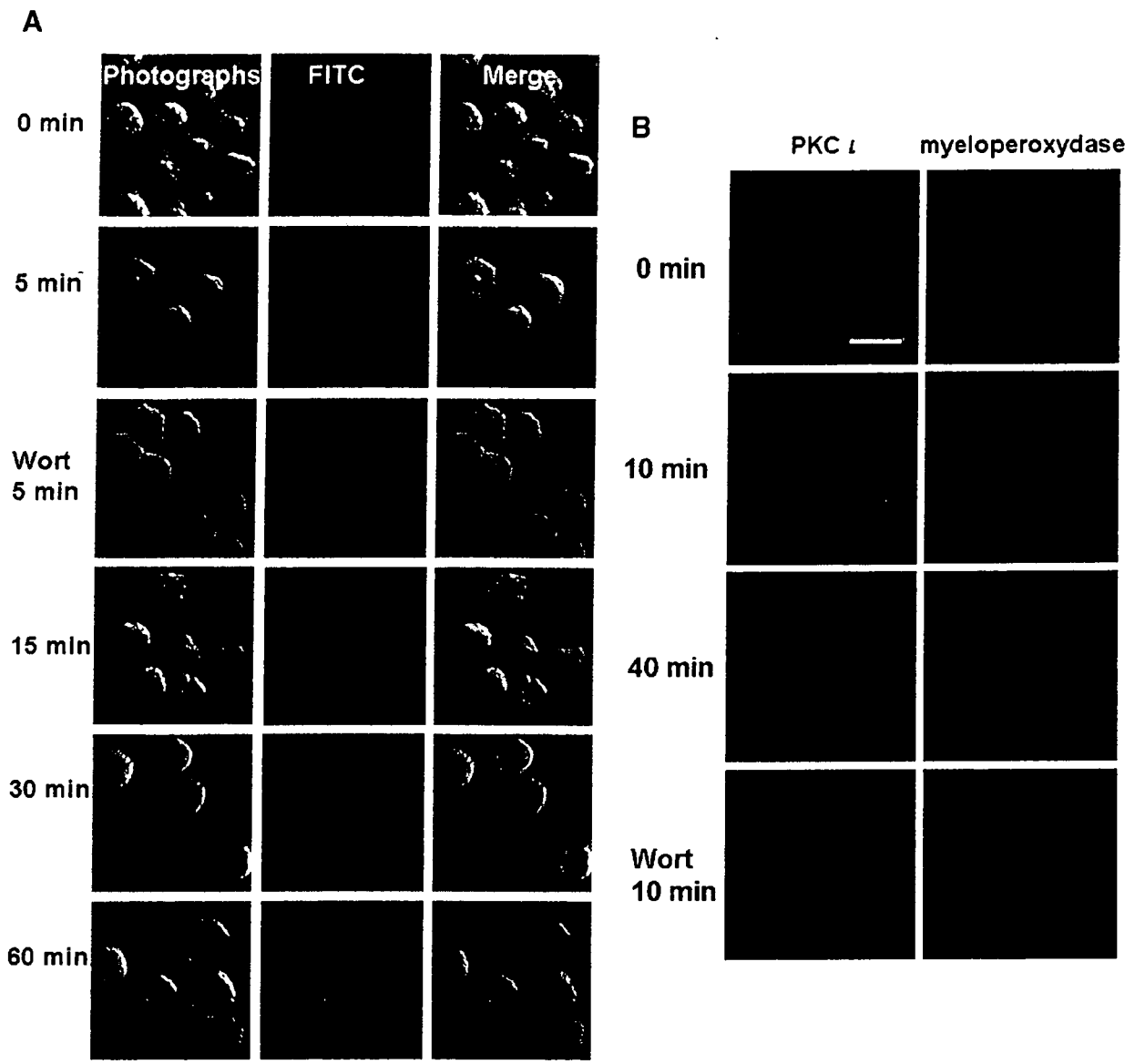

Fig. 3. Translocation of PKCι after the activation of G-CSF. A: 2 days after the addition of DMSO, HL-60 cells stimulated by G-CSF were fixed, incubated with anti-PKCι antibody, and visualized as described above. The photographs can be seen at the left part of the figure, the fluorescent photographs in the middle of the figure, and the merged images at the right. B: G-CSF-stimulated mononuclear cells from cord blood were stained with anti-PKCι antibody (red, left part) and anti-myeloperoxidase antibody (green, right part) after serum depletion. Under no stimulation, PKCι was observed in the nucleus. G-CSF promoted the translocation of PKCι to the membrane within 5–15 min, and then to the cytosol. Wort: wortmannin. White bar: 10 μm.

neutrophilic HL-60 cells, PKCι proteins were markedly expressed in these cells (Fig. 1B). This study showed, for the first time, the stimulation of PKCι activity in G-CSF-treated HL-60 cells (Fig. 2B) at 15–30 min after the addition of G-CSF. Maximum activation from the addition of NGF in PC12 cells was also observed at 15 min (Wooten et al., 2001).

Atypical PKCs are lipid-regulated kinases that need to be localized to the membrane in order to be activated. PKCζ is directly activated by phosphatidylinositol 3,4,5-trisphosphate, a product of PI3K (Nakanishi et al., 1993). We previously reported that the maximum activation of PI3K was observed in HL-60 cells 5 min after the addition of G-CSF (Kanayasu-Toyoda et al., 2002). Most investigators have reported the translocation of aPKC in either muscle cells or adipocytes stimulated by insulin (Andjelkovic et al., 1997; Goransson et al., 1998; Galetic et al., 1999; Standaert et al., 1999; Braiman et al., 2001; Chen et al., 2003; Kanzaki et al., 2004; Sasaoka et al., 2004; Herr et al., 2005). In response to insulin stimulation, aPKCζ/λ is translocated to the plasma membrane (Standaert et al., 1999; Braiman et al., 2001), where aPKCζ/λ is believed to be activated (Galetic et al., 1999; Kanzaki et al., 2004). In the present study, the addition of G-CSF induced PKCι to translocate to the membrane from the nucleus within 5–15 min (Figs. 3 and 4), and this translocation to the plasma membrane accompanied the full activation of PKCι (Fig. 2B). Previously we reported also that the maximum activation of p70 S6K in HL-60 cells was observed from 30 to 60 min after the addition of G-CSF (Kanayasu-Toyoda et al., 1999, 2002), suggesting that there was a time lag between the activation of PI3K and p70 S6K upon the addition of G-CSF in HL-60 cells. In the present study, PKCι was

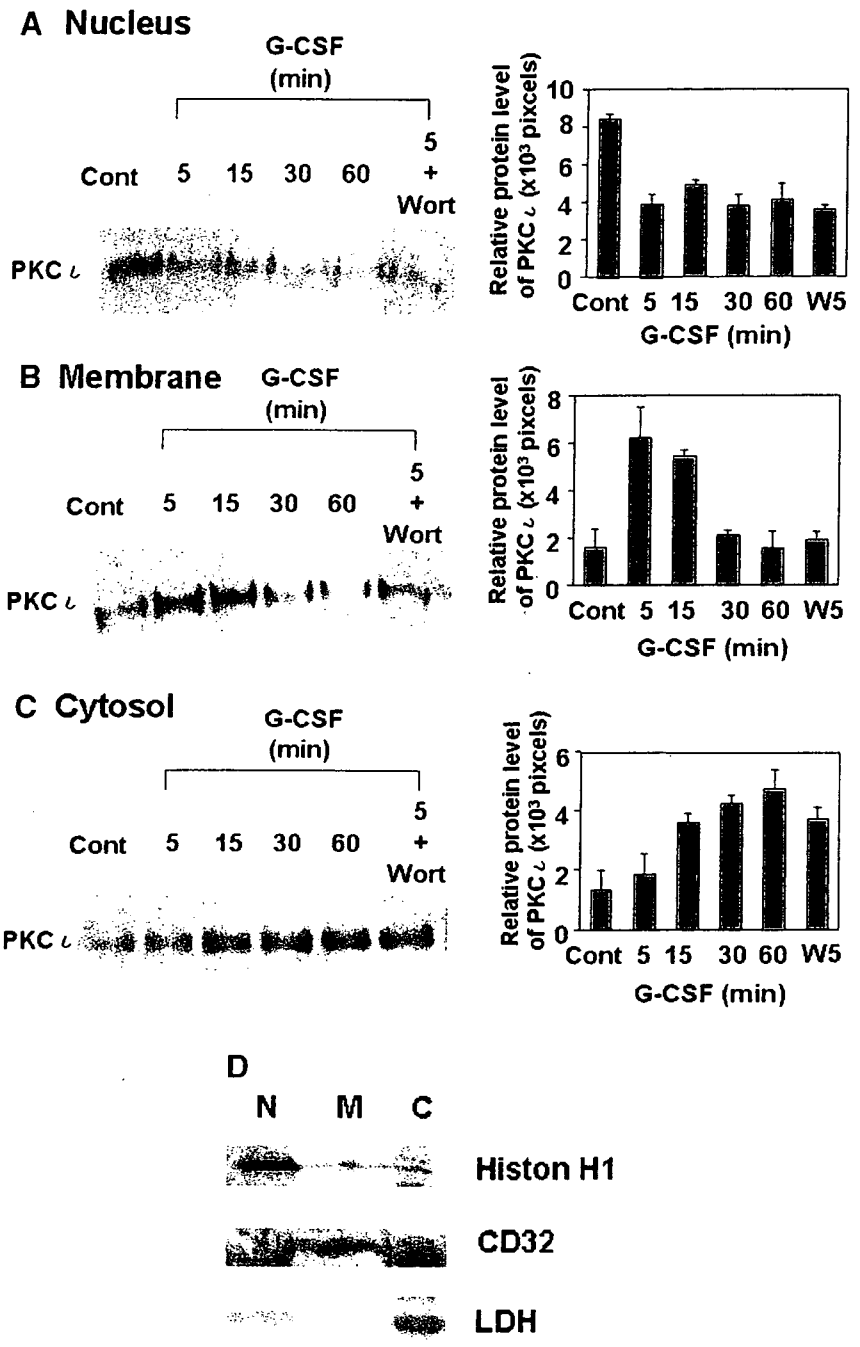

Fig. 4. Translocation of PKCι after activation by G-CSF on biochemical fractionation. The cells were differentiated as described in the Figure 3 legend. After stimulation by G-CSF, the amounts of PKCι proteins in the nucleus (A), plasma membrane (B), and cytosol (C), as fractionated by differential centrifugation, were analyzed by Western blotting (left parts). The right parts show the quantitation of the bands of PKCι proteins. Wort or W: wortmannin. PKCι protein was quantitated using data from three separate experiments. Columns and bars represent the mean ± SD. D: Each cell fraction was immunoblotted with antibodies of specific marker. Histon-H1, Fcγ receptor IIa (CD32), and lactate dehydrogenase (LDH) are specific markers for nuclear (N), membrane (M), and cytosolic (C) fractions, respectively.

found to re-translocate from the plasma membrane to the cytosol (Figs. 3 and 4C). In the presence of wortmannin, an inhibitor of PI3K, PKCι failed to translocate into the plasma membrane, but instead translocated to cytosol directly from the nucleus upon the addition of G-CSF (Figs. 3 and 4B). PKCι translocation was also observed in myeloperoxidase-positive cells derived from human cord blood (Fig. 3B), indicating that G-CSF-induced dynamic translocation of PKCι occurred in not only a limited cell line but also neutrophilic lineage cells. These data suggest that PI3K plays an important role in the activation and translocation of PKCι during the G-CSF-induced activation of myeloid cells. Furthermore, the translocation to the plasma membrane in response to G-CSF is wortmannin sensitive, but the translocation from the nucleus upon G-CSF stimulation is not affected by wortmannin, suggesting that the initial signal of G-CSF-induced PKCι translocation from the nucleus may be

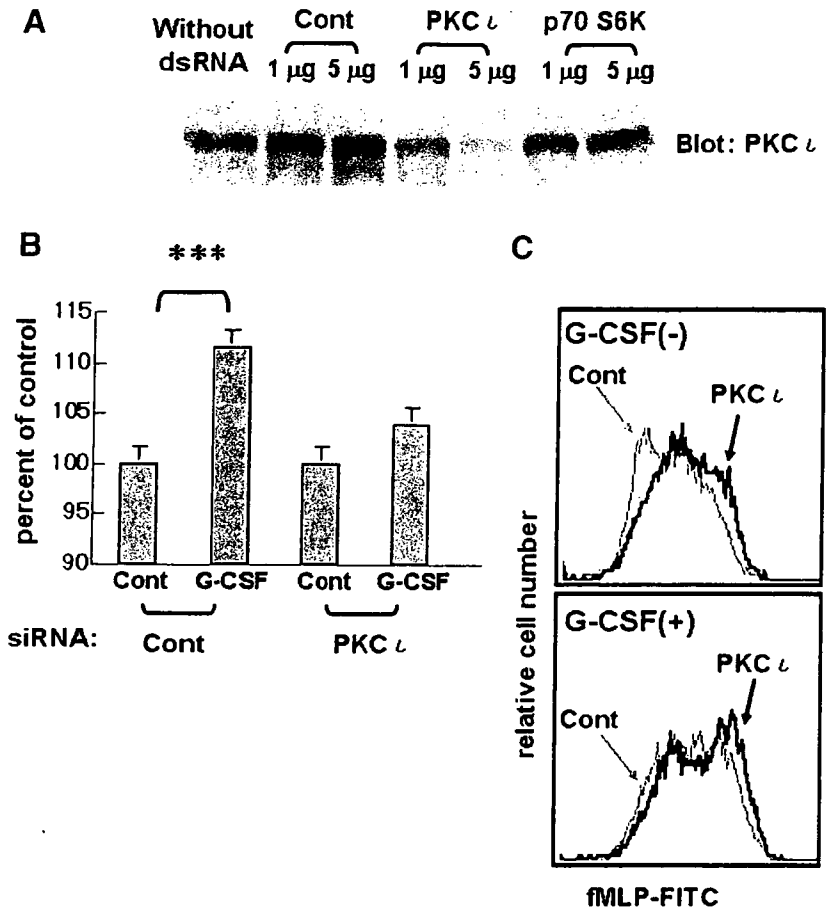

Fig. 5. Effects of siRNA of PKCι on proliferation, differentiation, and phosphorylation at various sites of p70 S6K. A: Forty-eight hours after transfection with siRNA of PKCι or p70 S6K, protein levels of PKCι were compared. B: Proliferation of the cells transfected with siRNA of PKCι or control (Cont) was measured 5 days after the addition of G-CSF. Columns and bars represent the mean ± SD of triplicate wells (*$P < 0.001$). C: fMLP-R expression was analyzed by flow cytometry 5 days after the addition of G-CSF. The gray arrow indicates cells transfected with the control sequence of double-stranded RNA (Cont, gray lines), and the black arrow the cells transfected with siRNA for PKCι (black lines) in the presence (lower part) or absence (upper part) of G-CSF.**

PI3K-independent, but association of PKCι with the plasma membrane could be mediated through a PI3K-dependent signal. Cord blood is an important material of blood transplantation for leukemia (Bradstock et al., 2006; Ooi, 2006; Yamada et al., 2006) or for congenital neutropenia (Mino et al., 2004; Nakazawa et al., 2004) because it contains many hematopoietic stem cells such as CD34-positive cells or CD133-positive cells, and also contains immature granulocytes. The neutrophilic differentiation and proliferation are necessary processes after transplantation.

Formyl-Met-Leu-Phe peptide evokes the migration, superoxide production, and phagocytosis of neutrophils through fMLP-R, a suitable marker for neutrophilic differentiation. In this study, the reduction of PKCι by siRNA inhibited G-CSF-induced proliferation (Fig. 5B) and promoted neutrophilic differentiation (Fig. 5C) in terms of fMLP-R expression. These data, however, suggest that PKCι promoted G-CSF-induced proliferation and blocked differentiation at the same time.

The substrates of aPKC have recently been reported: namely, the cytoskeletal protein Lethal giant larvae (Lgl) was phosphorylated by Drosophila aPKC (Betschinger et al., 2003) and glyceraldehydes-3-phosphate dehydrogenase (GAPDH) was phosphorylated by PKCι (Tisdale, 2002) directly in both cases. While the direct phosphorylation of p70 S6K by aPKC was not observed (Akimoto et al., 1998; Romanelli et al., 1999), the enzyme activity of p70 S6K was markedly enhanced by co-transfection with aPKC and PDK-1, the latter of which is recruited to the membrane due to the binding of phosphatidylinositol-3,4,5-trisphosphate to its PH domain (Anderson et al., 1998). The addition of G-CSF induced PKCι to increase phosphorylation at Thr-389, which is the site most closely related to enzyme activity among the multi-phosphorylation sites of p70 S6K (Weng et al., 1998). However, the mammalian target of rapamycin (mTOR), an upstream regulator, also phosphorylates Thr-389 of p70 S6K and markedly stimulates p70 S6K activity under coexistence with PDK-1 (Isotani et al., 1999). We could not rule out the possibility that other PKC isoforms can contribute to the activation of p70 S6K. We postulated that in G-CSF-stimulated HL-60 cells, PKCι contributes to p70 S6K activation as an upstream regulator.

Atypical PKC isoforms are reported to play an important role in the activation of IκB kinase β (Lallena et al., 1999). In PKCζ-deficient mice, impaired signaling through the B-cell receptor resulted in the inhibition of cell proliferation and survival while also causing defects in the activation of ERK and the transcription of NF-κB-dependent genes (Martin et al., 2002). Moreover, Lafuente et al. (2003) demonstrated that the loss of Par-4, that is, the genetic inactivation of the aPKC inhibitor, led to an increased proliferative response of

peripheral T cells when challenged through the T-cell receptor. However, it has been reported that PKCλ-deficient mice have a lethal phenotype at the early embryonic stage (Soloff et al., 2004). Based on the present results and those of previous reports (Kanayasu-Toyoda et al., 1999, 2002), we postulate that PKCι plays an important role in regulating G-CSF-induced proliferation in neutrophilic lineage cells.

Acknowledgments

We thank the Metro Tokyo Red Cross Cord Blood Bank (Tokyo, Japan) for their kind cooperation. This work was supported in part by a grand-in-aid for health and labor science research (H17-SAISEI-021) from the Japanese Ministry of Health, Labor and Welfare, and in part by a grand-in-aid for Research on Health Sciences focusing on Drug Innovation from the Japan Health Sciences Foundation.

Literature Cited

Akimoto K, Nakaya M, Yamanaka T, Tanaka J, Matsuda S, Weng QP, Avruch J, Ohno S. 1998. Atypical protein kinase Clambda binds and regulates p70 S6 kinase. Biochem J 335:417–424.

Anderson KE, Coadwell J, Stephens LR, Hawkins PT. 1998. Translocation of PDK-1 to the plasma membrane is important in allowing PDK-1 to activate protein kinase B. Curr Biol 8:684–691.

Andjelkovic M, Alessi DR, Meier R, Fernandez A, Lamb NJ, Frech M, Cron P, Cohen P, Lucocq JM, Hemmings BA. 1997. Role of translocation in the activation and function of protein kinase B. J Biol Chem 272:31515–31524.

Betschinger J, Mechtler K, Knoblich JA. 2003. The Par complex directs asymmetric cell division by phosphorylating the cytoskeletal protein Lgl. Nature 422:326–330.

Bradstock KF, Hertzberg MS, Kerridge IH, Svennilson J, McGurgan M, Huang G, Antonenas V, Gottlieb DJ. 2006. Unrelated umbilical cord blood transplantation for adults with haematological malignancies: Results from a single Australian centre. Intern Med J 36:355–361.

Braiman L, Alt A, Kuroki T, Ohba M, Bak A, Tennenbaum T, Sampson SR. 2001. Activation of protein kinase C zeta induces serine phosphorylation of VAMP2 in the GLUT4 compartment and increases glucose transport in skeletal muscle. Mol Cell Biol 21:7852–7861.

Chen X, Al-Hasani H, Olausson T, Wenthzel AM, Smith U, Cushman SW. 2003. Activity, phosphorylation state and subcellular distribution of GLUT4-targeted Akt2 in rat adipose cells. J Cell Sci 116:3511–3518.

Chuang LY, Guh JY, Liu SF, Hung MY, Liao TN, Chiang TA, Huang JS, Huang YL, Lin CF, Yang YL. 2003. Regulation of type II transforming-growth-factor-beta receptors by protein kinase C iota. Biochem J 375:385–393.

Chung J, Grammer TC, Lemon KP, Kazlauskas A, Blenis J. 1994. PDGF- and insulin-dependent p70 S6K activation mediated by phosphatidylinositol-3-OH kinase. Nature 370:71–75.

Debili N, Robin C, Schiavon V, Letestu R, Pflumio F, Mitjavila-Garcia MT, Coulombel L, Vainchenker W. 2001. Different expression of CD41 on human lymphoid and myeloid progenitors from adults and neonates. Blood 97:2023–2030.

Fritsch G, Buchinger P, Printz D, Fink FM, Mann G, Peters C, Wagner T, Adler A, Gadner H. 1993. Rapid discrimination of early CD34+ myeloid progenitors using CD45-RA analysis. Blood 81:2301–2309.

Galetic I, Andjelkovic M, Meier R, Brodbeck D, Park J, Hemmings BA. 1999. Mechanism of protein kinase B activation by insulin/insulin-like growth factor-1 revealed by specific inhibitors of phosphoinositide 3-kinase—Significance for diabetes and cancer. Pharmacol Ther 82:409–425.

Goransson O, Wijkander J, Manganiello V, Degerman E. 1998. Insulin-induced translocation of protein kinase B to the plasma membrane in rat adipocytes. Biochem Biophys Res Commun 246:249–254.

Hao QL, Zhu J, Price MA, Payne KJ, Barsky LW, Crooks GM. 2001. Identification of a novel, human multilymphoid progenitor in cord blood. Blood 97:3683–3690.

Herr HJ, Bernard JR, Reeder DW, Rivas DA, Limon JJ, Yaspelkis BB3rd. 2005. Insulin-stimulated plasma membrane association and activation of Akt2, aPKC zeta and aPKC lambda in high fat fed rodent skeletal muscle. J Physiol 565:627–636.

Huang S, Chen Z, Yu JF, Young D, Bashey A, Ho AD, Law P. 1999. Correlation between IL-3 receptor expression and growth potential of human CD34+ hematopoietic cells from different tissues. Stem Cells 17:265–272.

Isotani S, Hara K, Tokunaga C, Inoue H, Avruch J, Yonezawa K. 1999. Immunopurified mammalian target of rapamycin phosphorylates and activates p70 S6 kinase alpha in vitro. J Biol Chem 274:34493–34498.

Kanayasu-Toyoda T, Yamaguchi T, Uchida E, Hayakawa T. 1999. Commitment of neutrophilic differentiation and proliferation of HL-60 cells coincides with expression of transferrin receptor. Effect of granulocyte colony stimulating factor on differentiation and proliferation. J Biol Chem 274:25471–25480.

Kanayasu-Toyoda T, Yamaguchi T, Oshizawa T, Kogi M, Uchida E, Hayakawa T. 2002. Role of the p70 S6 kinase cascade in neutrophilic differentiation and proliferation of HL-60 cells—a study of transferrin receptor-positive and -negative cells obtained from dimethyl sulfoxide- or retinoic acid-treated HL-60 cells. Arch Biochem Biophys 405:21–31.

Kanayasu-Toyoda T, Yamaguchi T, Oshizawa T, Uchida E, Hayakawa T. 2003. The role of c-Myc on granulocyte colony-stimulating factor-dependent neutrophilic proliferation and differentiation of HL-60 cells. Biochem Pharmacol 66:133–140.

Kanzaki M, Mora S, Hwang JB, Saltiel AR, Pessin JE. 2004. Atypical protein kinase C (PKCzeta/lambda) is a convergent downstream target of the insulin-stimulated phosphatidylinositol 3-kinase and TC10 signaling pathways. J Cell Biol 164:279–290.

Lafuente MJ, Martin P, Garcia-Cao I, Diaz-Meco MT, Serrano M, Moscat J. 2003. Regulation of mature T lymphocyte proliferation and differentiation by Par-4. Embo J 22:4689–4698.

Lallena MJ, Diaz-Meco MT, Bren G, Paya CV, Moscat J. 1999. Activation of IkappaB kinase beta by protein kinase C isoforms. Mol Cell Biol 19:2180–2188.

Liu WS, Heckman CA. 1998. The sevenfold way of PKC regulation. Cell Signal 10:529–542.

Manz MG, Miyamoto T, Akashi K, Weissman IL. 2002. Prospective isolation of human clonogenic common myeloid progenitors. Proc Natl Acad Sci USA 99:11872–11877.

Martin P, Duran A, Minguet S, Gaspar ML, Diaz-Meco MT, Rennert P, Leitges M, Moscat J. 2002. Role of zeta PKC in B-cell signaling and function. Embo J 21:4049–4057.

Mino E, Kobayashi R, Yoshida M, Suzuki Y, Yamada M, Kobayashi K. 2004. Umbilical cord blood stem cell transplantation from unrelated HLA-matched donor in an infant with severe congenital neutropenia. Bone Marrow Transplant 33:969–971.

Muscella A, Greco S, Elia MG, Storelli C, Marsigliante S. 2003. PKC-zeta is required for angiotensin II-induced activation of ERK and synthesis of C-FOS in MCF-7 cells. J Cell Physiol 197:61–68.

Nakanishi H, Brewer KA, Exton JH. 1993. Activation of the zeta isozyme of protein kinase C by phosphatidylinositol 3,4,5-trisphosphate. J Biol Chem 268:13–16.

Nakazawa Y, Sakashita K, Kinoshita M, Saida K, Shigemura T, Yanagisawa R, Shikama N, Kamijo T, Koike K. 2004. Successful unrelated cord blood transplantation using a reduced-intensity conditioning regimen in a 6-month-old infant with congenital neutropenia complicated by severe pneumonia. Int J Hematol 80:287–290.

Nguyen BT, Dessauer CW. 2005. Relaxin stimulates protein kinase C zeta translocation: Requirement for cyclic adenosine 3′,5′-monophosphate production. Mol Endocrinol 19:1012–1023.

Ooi J. 2006. The efficacy of unrelated cord blood transplantation for adult myelodysplastic syndrome. Leuk Lymphoma 47:599–602.

Rappold I, Ziegler BL, Kohler I, Marchetto S, Rosnet O, Birnbaum D, Simmons PJ, Zannettino AC, Hill B, Neu S, Knapp W, Alitalo R, Alitalo K, Ullrich A, Kanz L, Buhring HJ. 1997. Functional and phenotypic characterization of cord blood and bone marrow subsets expressing FLT3 (CD135) receptor tyrosine kinase. Blood 90:111–125.

Romanelli A, Martin KA, Toker A, Blenis J. 1999. p70 S6 kinase is regulated by protein kinase Czeta and participates in a phosphoinositide 3-kinase-regulated signalling complex. Mol Cell Biol 19:2921–2928.

Sasaoka T, Wada T, Fukui K, Murakami S, Ishihara H, Suzuki R, Tobe K, Kadowaki T, Kobayashi M. 2004. SH2-containing inositol phosphatase 2 predominantly regulates Akt2, and not Akt1, phosphorylation at the plasma membrane in response to insulin in 3T3-L1 adipocytes. J Biol Chem 279:14835–14843.

Selbie LA, Schmitz-Peiffer C, Sheng Y, Biden TJ. 1993. Molecular cloning and characterization of PKC iota, an atypical isoform of protein kinase C derived from insulin-secreting cells. J Biol Chem 268:24296–24302.

Soloff RS, Katayama C, Lin MY, Feramisco JR, Hedrick SM. 2004. Targeted deletion of protein kinase C lambda reveals a distribution of functions between the two atypical protein kinase C isoforms. J Immunol 173:3250–3260.

Standaert ML, Bandyopadhyay G, Perez L, Price D, Galloway L, Poklepovic A, Sajan MP, Cenni V, Sirri A, Moscat J, Toker A, Farese RV. 1999. Insulin activates protein kinases C-zeta and C-lambda by an autophosphorylation-dependent mechanism and stimulates their translocation to GLUT4 vesicles and other membrane fractions in rat adipocytes. J Biol Chem 274:25308–25316.

Tenen DG, Hromas R, Licht JD, Zhang DE. 1997. Transcription factors, normal myeloid development, and leukemia. Blood 90:489–519.

Tisdale EJ. 2002. Glyceraldehyde-3-phosphate dehydrogenase is phosphorylated by protein kinase Ciota/lambda and plays a role in microtubule dynamics in the early secretory pathway. J Biol Chem 277:3334–3341.

Ward AC, Loeb DM, Soede-Bobok AA, Touw IP, Friedman AD. 2000. Regulation of granulopoiesis by transcription factors and cytokine signals. Leukemia 14:973–990.

Weng QP, Kozlowski M, Belham C, Zhang A, Comb MJ, Avruch J. 1998. Regulation of the p70 S6 kinase by phosphorylation in vivo. Analysis using site-specific anti-phosphopeptide antibodies. J Biol Chem 273:16621–16629.

Wooten MW, Vandenplas ML, Seibenhener ML, Geetha T, Diaz-Meco MT. 2001. Nerve growth factor stimulates multisite tyrosine phosphorylation and activation of the atypical protein kinase C's via a src kinase pathway. Mol Cell Biol 21:8414–8427.

Yamada K, Mizusawa M, Harima A, Kajiwara K, Hamaki T, Hoshi K, Kozai Y, Kodo H. 2006. Induction of remission of relapsed acute myeloid leukemia after unrelated donor cord blood transplantation by concomitant low-dose cytarabine and calcitriol in adults. Eur J Haematol 77:345–348.

Yamaguchi T, Mukasa T, Uchida E, Kanayasu-Toyoda T, Hayakawa T. 1999. The role of STAT3 in granulocyte colony-stimulating factor-induced enhancement of neutrophilic differentiation of Me2SO-treated HL-60 cells. GM-CSF inhibits the nuclear translocation of tyrosine-phosphorylated STAT3. J Biol Chem 274:15575–15581.

JCRB細胞バンク：厚生労働省

小原有弘，水澤 博〔独立行政法人 医薬基盤研究所 生物資源研究部 細胞資源研究室（JCRB細胞バンク）〕
機関名：独立行政法人 医薬基盤研究所 生物資源研究部 細胞資源研究室（JCRB細胞バンク）
URL：http://cellbank.nibio.go.jp/

Ⅰ．リソースの特徴

培養細胞は生命科学研究にとって必要不可欠な研究資源として十分に認識されており，非常に広範な研究に利用されるリソースとなっている．細胞は生物の最も基本的な構成単位であり，生命現象を再現できる最小単位が細胞であると言える．細胞は培養条件を制御することにより増殖させたり，機能を持った細胞へ分化させることも可能である．細胞を用いた研究は多岐に渡っているが大きく3つの研究に分けられる．第1に培養細胞を生体の模倣として使用し，培養細胞内で起こる事象を解析することで，生体内で起こっていることをより詳しく解明する研究．第2に遺伝子導入や遺伝子ノックアウトなど生体内とは異なる環境・状況を培養細胞で構築し，その解析を行うことで作り出した環境・状況が生体に与える影響を考える研究．第3に培養細胞を抗体産生や生理活性物質生産などのツールとして使用する研究．これら3つの研究において細胞が万能であるとは言えないが非常に有用な研究資源と言える．以前はよく増殖し，広く頒布しやすい癌細胞などの株化細胞が研究に広く利用されていたが，近年はヒトへの医療応用や治療法開発に向けて，機能や分化能をある程度維持したヒト由来の正常細胞や遺伝子導入細胞，不死化細胞の研究利用ニーズが高く，新たな研究資源の開発も進んでいる．

Ⅱ．リソースの整備状況

JCRB細胞バンクは1985年，厚生労働省（当時の厚生省）によって我が国初の細胞バンクとして設立され，生命科学研究全体の発展とともに細胞バンク事業も発展してきた．現在の登録細胞数は1,018種類（2007年6月）で，主にヒト由来細胞（622種類，61%）がコレクションされ厚生労働行政に資する研究に利用されている．また，2007年より京都大学放射線生物研究センターで収集された高発癌性遺伝病患者由来細胞1,999株（表1）の分譲を開始した．JCRB細胞バンクでは高品質な細胞提供を行っており，マイコプラズマなどの微生物汚染検査，細胞のクロスコンタミネーション（細胞の入れ替わり）などを検査する細胞個別識別検査，染色体解析，性状検査などの品質管理を実施し，ガラスアンプルに細胞を封入した状態で液体窒素保存容器に保管した

表1．高発癌性遺伝病患者由来細胞コレクション

疾患名	株数	疾患名	株数	疾患名	株数
網膜芽細胞腫	651	家族性白血病	23	甲状腺髄様癌	5
色素性乾皮症	411	ブルーム症候群	20	色素失調症	4
ファンコニ貧血	232	ポイツ・イエーガー症候群	19	色素異常症	4
再生不良性貧血	124	疣贅状表皮発育異常症	14	基底細胞母斑症候群	4
コケイン症候群	83	シップル症候群	13	肝芽腫	4
毛細血管拡張性運動失調症	82	ダウン症候群	12	ベックウィズ・ウィーデマン症候群	4
家族性大腸ポリポーシス	71	ロスムンド・トムソン症候群	9	その他	159
先天性異常・先天性奇形	43	ガードナー症候群	8		

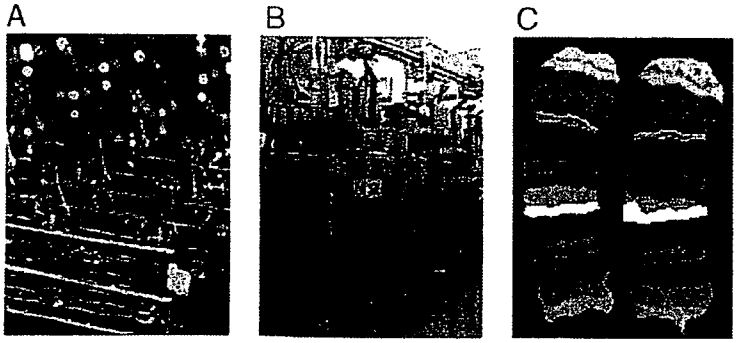

図1．JCRB細胞バンクでの細胞品質に関わる取り組み
A：高品質な細胞アンプル．
B：超低温（液体窒素）細胞凍結保存容器．
C：mBand法による染色体詳細解析．